Magnetoelasticity of highly deformable thin films: Theory and simulation

Matthew Barham, David Steigmann, Dan White

Magnetoelasticity of highly deformable thin films: Theory and simulation ☆

M. Barham [a,b], D.J. Steigmann [a,*], D. White [b]

[a] Mechanical Engineering, University of California, Berkeley, CA 94720, USA
[b] Lawrence Livermore National Laboratory, Livermore, CA 94550, USA

A B S T R A C T

A non linear two dimensional theory is developed for thin magnetoelastic films capable of large deformations. This is derived directly from the three dimensional theory. Significant simplifications emerge in the descent from three dimensions to two, permitting the self field generated by the body to be computed *a posteriori*. The model is specialized to isotropic elastomers and numerical solutions are obtained to equilibrium boundary value problems in which the membrane is subjected to lateral pressure and an applied magnetic field.

1. Introduction

There is considerable current interest among mechanicians in non linear magnetoelasticity [1 5]. This is due to the develop ment of highly deformable magnetizable materials synthesized from elastomers infused with micro or nano scopic ferrous particles [6]. Such materials are capable of large deformations induced by magnetic fields. This property may be used to facilitate controlled pumping of fluid, for example, via remote actuation. In the present work we continue our development [7] of a membrane theory for thin films composed of such materials. This is used to simulate membrane response to an applied magnetic field and to a pressure transmitted to the material by a confined gas.

Section 2 contains a summary of three dimensional magne toelasticity and its specialization to isotropic elastomers. A corresponding membrane model is derived in Section 3 directly from the equations of the three dimensional theory. It incorpo rates a constraint requiring the magnetization to remain tangen tial to the film as it deforms. This is motivated by the fact that such states are energetically optimal in thin films [8,9]. Likewise, we impose the constraint of bulk incompressibility, and thus exclude dilational modes of deformation that are energetically unfavorable in typical elastomers. However, unlike incompressi bility, the constraint on magnetization is not of the kind that requires a reactive Lagrange multiplier in the relevant constitu tive equation. Rather, it is a restriction involving the deformation, allowing local membrane geometry to adjust in response to an applied field. Constraints on the deformation of the Kirchhoff Love type are typically imposed at the outset in theories of thin magnetoelastic plates [10]. However, in general such constraints impede the attainment of minima of the overall energy because, by confining attention to states of magnetization that are optimal at any deformation, we effectively eliminate magnetization as an independent variable. The bias induced by an applied field then yields deformations that violate constraints of the Kirchhoff Love type. Here, this is addressed via a *director* field which emerges naturally from the underlying three dimensional theory in the manner described in [11] for the purely mechanical problem, without restricting the nature of the deformation in thin bodies.

In Section 4 we use a finite difference method to discretize the model spatially and discuss the solution of the resulting equations by the method of *dynamic relaxation*, in which equilibria are obtained as long time limits of solutions to an artificial dynamical system with viscosity. The method is applied, in Section 5, to determine the deformation, magnetization and magnetic field generated by a thin film in response to an applied dipole field and pressure load.

Notation follows standard usage in non linear continuum mechanics [12]. Thus, boldface is used to denote vectors and tensors, bold subscripts are used to denote derivatives with respect to the indicated tensor or vector variables, the superscript t is used to denote transposition, and the superscripts -1 and $-t$ to denote the inverse and inverted transpose. The symbol $\otimes$ refers to the tensor product of vectors. A dot between variables in bold face is used to denote the standard Euclidean inner product, and $|\cdot|$ refers to the induced norm.

2. Three-dimensional magnetoelasticity

The background material on continuum electromagnetism underlying this work may be found in [9,13 17]. We apply this

☆ For Ray Ogden, Prager Medalist.

* Corresponding author.
E-mail address: steigman@me.berkeley.edu (D.J. Steigmann).

to the description of incompressible magnetic elastomers undergoing large deformations. A summary of the relevant equations is given followed by discussions of restrictions associated with stable equilibria and the specialization of the theory to isotropic materials.

2.1. Basic equations

The local equation of motion in the absence of electric fields or applied (as distinct from electromagnetic) body forces is [9,17]

$$div\,\mathbf{T}=\rho\mathbf{y}\quad\text{in}\quad R, \tag{1}$$

where

$$\mathbf{T}=\rho(\xi_{\mathbf{F}})\mathbf{F}^t+\mu_0(\mathbf{h}\otimes\mathbf{h}\quad\tfrac{1}{2}|\mathbf{h}|^2\mathbf{I})+\mu_0\mathbf{h}\otimes\mathbf{m}\quad q\mathbf{I} \tag{2}$$

is the magnetoelastic Cauchy stress; $\xi(\mathbf{F},\mathbf{m})$ is the free energy per unit mass; ρ is the mass density (mass per unit current volume); $\mathbf{h}$ is the magnetic field; $\mathbf{m}$ is the magnetization per unit current volume; $\mathbf{F}=D\boldsymbol{\chi}$ is the gradient of the deformation function $\mathbf{y}=\boldsymbol{\chi}(\mathbf{x},t)$ in which $\mathbf{x}$ is the position of a material point in a fixed reference configuration κ and D is the gradient with respect to $\mathbf{x}$; superposed dots are used to denote material derivatives; R is the configuration occupied by the body at time t; and $\mu_0(>0)$ is the free space permeability. Here $\mathbf{I}$ is the unit tensor, *div* is the spatial divergence based on $\mathbf{y}$ and q is a Lagrange multiplier field associated with the incompressibility constraint.

Maxwell's equations may be used [9] to show that

$$div\{\mathbf{h}\otimes(\mathbf{h}+\mathbf{m})\quad\tfrac{1}{2}|\mathbf{h}|^2\mathbf{I}\}=(grad\,\mathbf{h})\mathbf{m}, \tag{3}$$

where *grad* is the gradient with respect to $\mathbf{y}$, and thus furnish an equivalent equation of motion:

$$div[\rho(\xi_{\mathbf{F}})\mathbf{F}^t\quad q\mathbf{I}]+\mu_0(grad\,\mathbf{h})\mathbf{m}=\rho\mathbf{y}, \tag{4}$$

which proves, for reasons discussed below, to be more convenient for our purposes. Here we have suppressed time derivatives in Maxwell's equations. This is justified in the absence of electric fields if, as assumed here, there are no free charges or currents and the body is not electrically polarized (see [17]).

If $\mathbf{t}_a$ is the applied (i.e, non electromagnetic) traction acting on a part ∂R_t of the boundary ∂R, then [9]

$$\rho(\xi_{\mathbf{F}})\mathbf{F}^t\mathbf{n}\quad q\mathbf{n}=\mathbf{t}_a+\tfrac{1}{2}\mu_0(\mathbf{m}\cdot\mathbf{n})^2\mathbf{n}\quad\text{on}\quad\partial R_t. \tag{5}$$

Typical boundary value problems, including those considered here, entail the assignment of $\mathbf{y}$ on the complement $\partial R\backslash\partial R_t$. This system is augmented by the incompressibility constraint

$$\rho(\boldsymbol{\chi}(\mathbf{x},t),t)=\rho_\kappa(\mathbf{x});\ \text{equivalently,}\quad J=1,\quad\text{where}\quad J=\det\mathbf{F}. \tag{6}$$

Our further considerations require equations involving a referential divergence operator. For (4), this is easily achieved via the Piola transformation:

$$\mathbf{P}=[\rho(\xi_{\mathbf{F}})\mathbf{F}^t\quad q\mathbf{I}]\mathbf{F}^*=W_{\mathbf{F}}\quad q\mathbf{F}^*, \tag{7}$$

where

$$W(\mathbf{F},\mathbf{m})=\rho_\kappa\xi \tag{8}$$

is the referential strain energy density, and

$$\mathbf{F}^*=J\mathbf{F}^{-t} \tag{9}$$

is the cofactor of the deformation gradient. Thus,

$$J\,div[\rho(\xi_{\mathbf{F}})\mathbf{F}^t\quad q\mathbf{I}]=Div\,\mathbf{P}, \tag{10}$$

where *Div* is the referential divergence based on $\mathbf{x}$; therefore, (4) is equivalent to

$$Div\,\mathbf{P}+\mu_0(grad\,\mathbf{h})\mathbf{m}=\rho_\kappa\mathbf{y}, \tag{11}$$

in which $J=1$ has been imposed. Further, we find the referential form of the boundary condition (5) to be

$$\mathbf{PN}=\mathbf{p}_a+\tfrac{1}{2}\mu_0(\mathbf{m}\cdot\mathbf{n})^2\mathbf{F}^*\mathbf{N}\quad\text{on}\quad\partial\kappa_t, \tag{12}$$

where $\partial R_t=\chi(\partial\kappa_t)$, having used Nanson's formula:

$$\alpha\mathbf{n}=\mathbf{F}^*\mathbf{N}, \tag{13}$$

where $\alpha=|\mathbf{F}^*\mathbf{N}|$ is the local areal dilation of $\partial\kappa_t$. Here,

$$\mathbf{p}_a=\alpha\mathbf{t}_a \tag{14}$$

is the applied traction measured per unit area of $\partial\kappa_t$.

The magnetic field is the sum [9]

$$\mathbf{h}=\mathbf{h}_a+\mathbf{h}_s \tag{15}$$

of an applied field $\mathbf{h}_a$, generated by remote sources, and the *self field* $\mathbf{h}_s$ generated by the magnetized body. In the present circumstances both satisfy the relevant Maxwell equation with out time derivatives; thus

$$curl\,\mathbf{h}_a=\mathbf{0} \tag{16}$$

in all of three space, denoted by $\mathcal{E}$, where *curl* is the spatial curl operation based on $\mathbf{y}$, whereas

$$curl\,\mathbf{h}_s=\mathbf{0} \tag{17}$$

in $\mathcal{E}\backslash\partial R$. The self field and the magnetization are subject to the jump condition [9]:

$$[\mathbf{h}_s]=(\mathbf{n}\cdot\mathbf{m})\mathbf{n}\quad\text{on}\quad\partial R, \tag{18}$$

where $[\cdot]$ is the difference between the exterior and interior limits of the enclosed variable on ∂R, and to Maxwell's equation [9]:

$$div\,\mathbf{h}_s=\quad div\,\mathbf{m}\quad\text{in}\quad R=0,\quad\text{and}\quad\text{in}\quad\mathcal{E}\backslash\overline{R}. \tag{19}$$

The field $\mathbf{h}_a$ is assumed to be assigned as a function that is continuously differentiable everywhere in $\mathcal{E}$ except at a finite number of singularities in $\mathcal{E}\backslash\overline{R}$.

In the examples discussed in Section 5 we study the response of the material to an applied field generated by a dipole source with the poles aligned along a fixed unit vector $\mathbf{k}$. Accordingly [7],

$$\mathbf{h}_a(\mathbf{y})=\tfrac{D}{\ell^3}[3(\mathbf{a}\cdot\mathbf{k})\mathbf{a}\quad\mathbf{k}], \tag{20}$$

where the (signed) constant D is the dipole strength, ℓ is the distance from the source to the point with position $\mathbf{y}\in\mathcal{E}$, and

$$\ell\mathbf{a}=\mathbf{y}\quad\mathbf{y}_d, \tag{21}$$

in which $|\mathbf{a}|=1$, is position measured from the source, located at $\mathbf{y}_d$. This has an isolated singularity at the source. The associated gradient, required in (11), is [7]

$$grad\,\mathbf{h}_a=3D\ell^{-4}\{[(\mathbf{a}\cdot\mathbf{k})\mathbf{I}+\mathbf{a}\otimes\mathbf{k}]\boldsymbol{\Pi}\quad[3(\mathbf{a}\cdot\mathbf{k})\mathbf{a}\quad\mathbf{k}]\otimes\mathbf{a}\},$$
$$\text{where}\quad\boldsymbol{\Pi}=\mathbf{I}\quad\mathbf{a}\otimes\mathbf{a}, \tag{22}$$

and is symmetric in accordance with (16).

From (17) (19) we have

$$\mathbf{h}_s=\quad grad\,\varphi_s, \tag{23}$$

where the scalar field φ_s satisfies

$$[grad\,\varphi_s]=\quad(\mathbf{n}\cdot\mathbf{m})\mathbf{n}\quad\text{on}\quad\partial R \tag{24}$$

and the *magnetostatic equation*:

$$div(grad\,\varphi_s)=div\,\mathbf{m}\quad\text{in}\quad R=0,\quad\text{and}\quad\text{in}\quad\mathcal{E}\backslash\overline{R}. \tag{25}$$

At any given time the unique solution satisfying $\varphi_s\sim|\mathbf{y}|^{-1}$ as $|\mathbf{y}|\to\infty$ is [14,16]

$$4\pi\varphi_s(\mathbf{y})=\int_{\partial R}\frac{\mathbf{m}(\mathbf{y}')\cdot\mathbf{n}(\mathbf{y}')}{|\mathbf{y}\quad\mathbf{y}'|}da(\mathbf{y}')\quad\int_R\frac{div\,\mathbf{m}(\mathbf{y}')}{|\mathbf{y}\quad\mathbf{y}'|}dv(\mathbf{y}')\quad\text{for}\quad\mathbf{y}\notin\partial R. \tag{26}$$

The magnetization and magnetic field are related constitutively by [9]

$$W_{\mathbf{m}} = \mu_0 \mathbf{h} = \mu_0 (\mathbf{h}_a \quad grad\ \varphi_s). \tag{27}$$

Thus, if the constitutive function $W(\mathbf{F},\mathbf{m})$ is known, Eqs. (11) (14) and (23), (26), (27) yield a coupled integro differential system to be solved for the deformation and magnetization. This presents considerable analytical and numerical challenges [18]. In [7] these were avoided by considering the limit of a weakly magnetized body in the presence of a strong applied field. In this limit the self field may be generated from (26) *a posteriori*, and plays only a passive role in the analysis. Alternatively, a direct simulation of the field may be based on a discretization of Maxwell's equations in the space surrounding the body [4,19]. In Section 3 we use a result derived in [8] for thin films to show that the tractability of the formulation adopted in [7] is retained when the magnetization and applied fields are comparable in magnitude. This yields a conventional differential algebraic system to be solved on a reference surface associated with the thin film.

To facilitate subsequent analysis, we use a pull back $\mathbf{M}$ of $\mathbf{m}$ defined by

$$\int_s \mathbf{m}\cdot\mathbf{n}\, da = \int_S \mathbf{M}\cdot\mathbf{N}\, dA, \tag{28}$$

in which $S \subset \kappa$ is an arbitrary orientable surface and $s = \chi(S,t) \subset R$ is its image in the current configuration. Nanson's formula then furnishes

$$\mathbf{M} = J\mathbf{F}^{-1}\mathbf{m}. \tag{29}$$

In particular, this yields the convenient connections

$$\alpha\mathbf{m}\cdot\mathbf{n} = \mathbf{M}\cdot\mathbf{N} \quad \text{and} \quad J\, div\, \mathbf{m} = Div\, \mathbf{M}, \tag{30}$$

which enable us to use, in place (12) and (26), respectively, the equivalent expressions

$$\mathbf{PN} = \mathbf{p}_a + \tfrac{1}{2}\mu_0\alpha^{-2}(\mathbf{M}\cdot\mathbf{N})^2\mathbf{F}^{*}\mathbf{N} \quad \text{on} \quad \partial\kappa_t \tag{31}$$

and

$$4\pi\varphi_s(\mathbf{y},t) = \int_{\partial\kappa} \frac{\mathbf{M}(\mathbf{x},t)\cdot\mathbf{N}(\mathbf{x})}{|\mathbf{y} \quad \boldsymbol{\chi}(\mathbf{x},t)|} dA(\mathbf{x}) \quad \int_{\kappa} \frac{Div\, \mathbf{M}(\mathbf{x},t)}{|\mathbf{y} \quad \boldsymbol{\chi}(\mathbf{x},t)|} dV(\mathbf{x}), \quad \text{for} \quad \mathbf{x}\notin\partial\kappa, \tag{32}$$

in which the role of time has been made explicit and incompressibility has been imposed.

2.2. Stability and strong ellipticity

A magneto mechanical energy balance may be derived from (11), (12), (18), (19). Thus [9,20],

$$\frac{d}{dt}\left\{K + \int_R \rho\xi\, dv + M \quad \mu_0 \int_R \mathbf{h}_a\cdot\mathbf{m}\, dv\right\} = \int_{\partial R_t} \mathbf{t}_a\cdot\dot{\mathbf{y}}\, da, \tag{33}$$

where

$$K = \frac{1}{2}\int_R \rho|\dot{\mathbf{y}}|^2\, dv \tag{34}$$

is the conventional kinetic energy and [3,9,15,16]

$$M = \quad \frac{1}{2}\mu_0 \int_R \mathbf{h}_s\cdot\mathbf{m}\, dv \tag{35}$$

is the *magnetostatic energy* of the self field. In this work we consider conservative applied tractions for which

$$\int_{\partial R_t} \mathbf{t}_a\cdot\dot{\mathbf{y}}\, da = \frac{d}{dt}L, \tag{36}$$

where L is a suitable load potential. We then have the conservation law

$$\tfrac{d}{dt}E' = 0, \quad \text{where} \quad E' = K + E \tag{37}$$

is the total magneto mechanical energy in which

$$E = \int_R \rho\xi\, dv + M \quad \mu_0 \int_R \mathbf{h}_a\cdot\mathbf{m}\, dv \quad L \tag{38}$$

is the magnetoelastic potential energy. We remark that our energy balance excludes certain terms that are present in the balance discussed in [20]. These vanish collectively when the applied field is assigned as a stationary function of $\mathbf{y}$, as assumed here; that is, as a function which is independent of t in the spatial description [9]. Further, the results of [9] may be used to show that the static specialization of (11), in which inertia is suppressed, furnishes an Euler Lagrange equation for E.

In this work we consider pressure acting on a part ∂R_t of the boundary formed by the union of two surfaces, ∂R_t^+ and ∂R_t^-, having no points in common. Uniformly distributed pressures, P^+ and P^-, respectively, are acting on these surfaces. Let S be a fixed orientable surface such that $\partial S = C$, the curve bounding ∂R_t^-. We choose S such that its closure, and that of ∂R_t^-, intersect only in C, so that $S \cup \partial R_t^-$ encloses a well defined volume $V^- \subset \mathcal{E}$. In the applications of interest here, ∂R_t^+ and ∂R_t^-, respectively are the 'upper' and 'lower' lateral surfaces of a thin sheet which, together with S, contains a compressible gas that transmits a pressure P^- to the lower surface. In Section 5 we identify S with the reference plane for the sheet. The upper surface is subjected to a fixed pressure P^+ supplied by a large reservoir.

This loading is conservative, and the associated potential, modulo an unimportant constant, is [9]

$$L = \int^{V} P^-(v)\, dv \quad P^+(V+V^-), \tag{39}$$

where $P^-(V^-)$ is the pressure volume relation for the compressible gas and V is the volume of the body in configuration R. In the present context, the incompressibility of the magnetoelastic material allows us to suppress V on the right hand side. Further,

$$V^- = \quad \frac{1}{3}\int_{\partial\kappa_t^-} \mathbf{y}\cdot\mathbf{F}^{*}\mathbf{N}\, dA, \tag{40}$$

where $\partial\kappa_t^-$ is the pre image of ∂R_t^- in the reference configuration with *exterior* unit normal $\mathbf{N}$ [9].

In a full thermodynamic treatment accounting for dissipative effects, the energy balance (37) is replaced by the imbalance $dE'/dt \le 0$ [20], so that if a state with vanishing initial velocity tends asymptotically to an equilibrium state, then the latter minimizes the potential energy E [5,20]; i.e., it furnishes a value of the potential energy not exceeding that supplied by the initial state. Because K is a positive definite function of the velocity, it follows that E' delivers a Lyapunov function for the dynamical system provided that the potential energy is strictly minimized at the equilibrium state. The considered equilibrium state is then stable. Without further qualification, this claim applies rigorously only to finite dimensional systems [21]. Thus, we apply it only to the system that has been discretized for the purpose of numerical analysis. This is the basis of a *dynamic relaxation* method for computing equilibria (Section 5).

In particular, then, an asymptotically stable equilibrium state minimizes the potential energy. In the purely mechanical setting, it is well known that a minimizing deformation necessarily satisfies the (local) strong ellipticity inequality pointwise (see, for example, [22]). In the present setting this is replaced by the magnetoelastic strong ellipticity inequalities [5]:

$$\mathbf{a}\cdot\mathbf{A}(\mathbf{b})\mathbf{a} > 0 \quad \text{and} \quad \mathbf{c}\cdot(W_{\mathbf{mm}})\mathbf{c} > 0, \tag{41}$$

where $\mathbf{A}(\mathbf{b})$ is the acoustic tensor defined by

$$\mathbf{a}\cdot\mathbf{A}(\mathbf{b})\mathbf{a}=\mathbf{a}\otimes\mathbf{b}\cdot\{W_{\mathbf{FF}}\quad W_{\mathbf{Fm}}(W_{\mathbf{mm}})^{-1}W_{\mathbf{mF}}\}[\mathbf{a}\otimes\mathbf{b}]. \tag{42}$$

These inequalities apply for all non zero vectors $\mathbf{a},\mathbf{b},\mathbf{c}$, with $\mathbf{a}$ and $\mathbf{b}$ subject to the restriction:

$$\mathbf{a}\cdot\mathbf{F}^{*}\mathbf{b}=0 \tag{43}$$

associated with incompressibility. The second inequality implies that $W_{\mathbf{mm}}$ is invertible, as required by the first inequality. In terms of Cartesian components, inequalities $(41)_{1,2}$ are

$$A_{ij}(\mathbf{b})a_ia_j>0\quad\text{and}\quad(\partial^2W/\partial m_i\partial m_j)c_ic_j>0, \tag{44}$$

where

$$A_{ij}(\mathbf{b})=\{\partial^2W/\partial F_{iA}\partial F_{jB}\quad(\partial^2W/\partial F_{iA}\partial m_k)(W_{\mathbf{mm}})^{-1}_{kl}(\partial^2W/\partial m_l\partial F_{jB})\}b_Ab_B. \tag{45}$$

They furnish pointwise restrictions on energy minimizing states of deformation and magnetization jointly, which in turn play a central role in reducing the three dimensional theory to a two dimensional membrane model (Section 3).

2.3. Reduced constitutive equations and isotropic materials

Balance of moment of momentum requires that the Cauchy stress tensor be symmetric in the absence of electric fields [14,17]. Using (2), the symmetry requirement may be reduced to the statement:

$$(W_{\mathbf{F}})\mathbf{F}^t+W_{\mathbf{m}}\otimes\mathbf{m}\quad\text{is symmetric,} \tag{46}$$

which is found, following [7], to be equivalent to the requirement:

$$W(\mathbf{F},\mathbf{m})=W(\mathbf{QF},\mathbf{Qm})\quad\text{for all rotations }\mathbf{Q}, \tag{47}$$

and this in turn is satisfied if and only if [7]

$$W(\mathbf{F},\mathbf{m})=\overline{W}(\mathbf{C},\overline{\mathbf{M}}) \tag{48}$$

for some function $\overline{W}$, where

$$\mathbf{C}=\mathbf{F}^t\mathbf{F}\quad\text{and}\quad\overline{\mathbf{M}}=\mathbf{F}^t\mathbf{m}. \tag{49}$$

The latter is related to the pull back $\mathbf{M}$ by (cf. (29))

$$J\overline{\mathbf{M}}=\mathbf{CM}, \tag{50}$$

and so W may be written as a (different) function of $\mathbf{C}$ and $\mathbf{M}$, if desired. We make use of this function in Section 3.

We assume the material to be isotropic, with a center of symmetry, relative to the reference configuration κ. Then [7]

$$\overline{W}(\mathbf{C},\overline{\mathbf{M}})=\overline{W}(\mathbf{R}^t\mathbf{CR},\mathbf{R}^t\overline{\mathbf{M}})\quad\text{for all orthogonal }\mathbf{R}. \tag{51}$$

For $\mathbf{R}=-\mathbf{I}$ this yields $\overline{W}(\mathbf{C},\overline{\mathbf{M}})=\overline{W}(\mathbf{C},-\overline{\mathbf{M}})$, which is satisfied if and only if [9] $\overline{W}(\mathbf{C},\overline{\mathbf{M}})=\hat{W}(\mathbf{C},\overline{\mathbf{M}}\otimes\overline{\mathbf{M}})$ for some function $\hat{W}$ subject to the restriction:

$$\hat{W}(\mathbf{C},\overline{\mathbf{M}}\otimes\overline{\mathbf{M}})=\hat{W}(\mathbf{R}^t\mathbf{CR},\mathbf{R}^t(\overline{\mathbf{M}}\otimes\overline{\mathbf{M}})\mathbf{R})\quad\text{for all orthogonal }\mathbf{R}. \tag{52}$$

For incompressible materials, standard representation theory [23] implies that $\hat{W}=U(I_1,I_2,I_4\quad I_6)$ for some function U, where

$$I_1=\mathrm{tr}\mathbf{C},\quad I_2=\tfrac{1}{2}[I_1^2\quad\mathrm{tr}(\mathbf{C}^2)],\ I_4=\mathbf{C}\cdot\overline{\mathbf{M}}\otimes\overline{\mathbf{M}},$$
$$I_5=\mathbf{C}^2\cdot\overline{\mathbf{M}}\otimes\overline{\mathbf{M}},\ I_6=\overline{\mathbf{M}}\cdot\overline{\mathbf{M}}. \tag{53}$$

Proceeding as in [9] we then obtain

$$W_{\mathbf{F}}=2\mathbf{F}(Sym\,\overline{W}_{\mathbf{C}})+\mathbf{m}\otimes\overline{W}_{\overline{\mathbf{M}}}\quad\text{and}\quad W_{\mathbf{m}}=\mathbf{F}\overline{W}_{\overline{\mathbf{M}}}, \tag{54}$$

with

$$Sym\,\overline{W}_{\mathbf{C}}=(U_1\quad I_1U_2)\mathbf{I}+U_2\mathbf{C}+U_4\overline{\mathbf{M}}\otimes\overline{\mathbf{M}}+U_5[\mathbf{C}(\overline{\mathbf{M}}\otimes\overline{\mathbf{M}})+(\overline{\mathbf{M}}\otimes\overline{\mathbf{M}})\mathbf{C}]$$
$$\text{and}\quad\overline{W}_{\overline{\mathbf{M}}}=2(U_4\mathbf{C}+U_5\mathbf{C}^2+U_6\mathbf{I})\overline{\mathbf{M}}, \tag{55}$$

where $U_k=\partial U/\partial I_k$.

To use this formalism we adopt a magnetoelastic extension of the classical Mooney–Rivlin strain energy function proposed in [5] and defined by

$$U=\tfrac{\mu}{2}\{(C_{10}+C_{11}J_1/\overline{M}_s^2)(I_1\quad3)+(C_{20}+C_{21}J_1/\overline{M}_s^2)(I_2\quad3)$$
$$+C_{01}J_1/\overline{M}_s^2+C_{02}J_2/\overline{M}_s^2+C_{01}^{*}[\cosh(J_1/\overline{M}_s^2)\quad1]\}, \tag{56}$$

where

$$J_1=I_5\quad I_1I_4+I_2I_6\quad\text{and}\quad J_2=I_6, \tag{57}$$

in which $\det\mathbf{F}=1$ has been imposed. Here μ is the ground state shear modulus, $\overline{M}_s$ is the saturation value of magnetization per unit volume, and the C_{ij} are dimensionless constants. Numerical values of μ, C_{ij} and $\mu_0\overline{M}_s$ are given in Ref. [5, Table 2], where μ_0 is the free space permeability. The symbols $J_{1,2}$ are used in [5] to denote invariants based on magnetization per unit mass. These are recovered on dividing our invariants by ρ_κ^2, and (56) takes this adjustment into account. Further, we have used $(49)_2$ and (53) to express the invariants adopted in [5], here based on magnetization per unit volume, in terms of the I_k. In [5] it is claimed that (56) satisfies $(41)_1$ without qualification. This comports with the fact that the standard Mooney–Rivlin model satisfies the purely mechanical strong ellipticity condition at all deformations [24]. Inequality $(41)_2$ was also shown in [5] to be satisfied over a substantial range of strain.

3. Membrane approximation

We consider a body whose reference configuration κ is a prismatic region generated by the parallel translation of a simply connected plane Ω with piecewise smooth boundary curve $\partial\Omega$. The closure of κ is $\overline{\Omega}\times[-h/2,h/2]$, where $\overline{\Omega}=\Omega\cup\partial\Omega$ and h is the (uniform) thickness. Let l be another length scale such as the diameter of a hole in Ω or a typical spanwise dimension. We assume that $\epsilon\doteq h/l\ll1$, and, in the theoretical development, adopt l as the unit of length ($l=1$). We derive a two dimensional membrane model by estimating the equations of the three dimensional theory to leading order in ϵ. Further, we suppose the deformation to be C^2 and the magnetization to be C^1 in the interior of the body, so that the local equations of the foregoing theory apply almost everywhere.

With minor loss of generality we assume the dipole in (20) to be orthogonal to the plane Ω, which is thus oriented by the unit vector $\mathbf{k}$. The projection onto the plane is

$$\mathbf{1}=\mathbf{I}\quad\mathbf{k}\otimes\mathbf{k} \tag{58}$$

and generates the orthogonal decomposition

$$\mathbf{P}=\mathbf{P1}+\mathbf{Pk}\otimes\mathbf{k} \tag{59}$$

of the Piola transform (7). Let ς be a linear coordinate in the direction of $\mathbf{k}$, and suppose $\varsigma=0$ on Ω. Eq. (11) is then equivalent to

$$Div_{\parallel}(\mathbf{P1})+\mathbf{P}'\mathbf{k}+\mu_0(grad\,\mathbf{h})\mathbf{m}=\rho_\kappa\mathbf{y}, \tag{60}$$

where $(\cdot)'=\partial(\cdot)/\partial\varsigma$ and $Div_{\parallel}$ is the (referential) *two dimensional* divergence with respect to position $\mathbf{u}$ on Ω, where

$$\mathbf{x}=\mathbf{u}+\varsigma\mathbf{k}. \tag{61}$$

This holds at all points in the interior of the body and therefore at $\varsigma=0$ in particular. Thus,

$$Div_{\parallel}(\mathbf{P}_0\mathbf{1})+\mathbf{P}_0'\mathbf{k}+\mu_0(grad\,\mathbf{h})_0\mathbf{m}_0=\rho_{\kappa0}\mathbf{y}_0, \tag{62}$$

where the subscript 0 identifies the values of functions at $\varsigma=0$; i.e., on the plane Ω. For example,

$$\mathbf{P}_0=W_{\mathbf{F}}(\mathbf{F}_0,\mathbf{m}_0)\quad q_0\mathbf{F}_0^{*}\quad\text{and}\quad\mu_0\mathbf{h}_0=W_{\mathbf{m}}(\mathbf{F}_0,\mathbf{m}_0) \tag{63}$$

in which [11]

$$\mathbf{F}_0 = \mathbf{f} + \mathbf{d} \otimes \mathbf{k}, \tag{64}$$

where

$$\mathbf{f} = \nabla \mathbf{r}, \tag{65}$$

$\mathbf{r}(\mathbf{u},t)(=\mathbf{y}_0)$ and $\mathbf{d}(\mathbf{u},t)$ are the restrictions to Ω of $\boldsymbol{\chi}$ and $\boldsymbol{\chi}'$, respectively, and ∇ is the two dimensional gradient on Ω; i.e., the gradient with respect to $\mathbf{u}$. We note that $\mathbf{r}(\mathbf{u},t)$ maps Ω to the deformed membrane surface $\omega = \chi(\Omega,t)$. Accordingly, $\mathbf{f}$ maps Ω', the translation space associated with the plane Ω, to T_ω, the tangent plane to ω at the material point $\mathbf{u} \in \Omega$.

To accommodate the constraint of bulk incompressibility we impose

$$1 = \det \mathbf{F}_0 = \mathbf{F}_0^* \mathbf{k} \cdot \mathbf{F}_0 \mathbf{k} = \alpha \mathbf{n} \cdot \mathbf{d}, \tag{66}$$

where (64) and Nanson's formula (13) have been used in the final equality. Here, α is the local areal dilation of Ω and $\mathbf{n}$ is the orientation of the surface onto which Ω is deformed; i.e., the unit normal to T_ω. The general solution is

$$\mathbf{d} = \alpha^{-1}\mathbf{n} + \mathbf{f}\mathbf{e}, \tag{67}$$

where $\mathbf{e} \in \Omega'$ is arbitrary. Further, Eqs. (13) and (64) yield

$$\alpha \mathbf{n} = \mathbf{f}\mathbf{i}_1 \times \mathbf{f}\mathbf{i}_2, \tag{68}$$

where $\mathbf{i}_\alpha \in \Omega'$ are subject only to the requirement that $\{\mathbf{i}_1, \mathbf{i}_2, \mathbf{k}\}$ be a positively oriented orthonormal set. Thus $\mathbf{F}_0$ is determined by $\mathbf{f}$ and $\mathbf{e}$, regarded as independent variables. The associated Cauchy Green deformation tensor, $\mathbf{C}_0 = \mathbf{F}_0^t \mathbf{F}_0$, is

$$\mathbf{C}_0 = \mathbf{c} + \mathbf{c}\mathbf{e} \otimes \mathbf{k} + \mathbf{k} \otimes \mathbf{c}\mathbf{e} + (\alpha^{-2} + \mathbf{e} \cdot \mathbf{c}\mathbf{e})\mathbf{k} \otimes \mathbf{k},$$
$$\text{where} \quad \mathbf{c} = \mathbf{f}^t \mathbf{f} \tag{69}$$

and α is obtained by evaluating the norm of (68), yielding

$$\alpha = \sqrt{\det \mathbf{c}}. \tag{70}$$

3.1. The leading order model

The foregoing equations, holding on Ω, are exact consequences of the three dimensional theory. Approximations arise in using them to represent material response in $\Omega \times [\ -\epsilon/2, \epsilon/2]$. Let $\mathbf{P}^{\pm}$ be the interior limits of $\mathbf{P}$ as $\varsigma \to \pm\epsilon/2$, where the exterior unit normals are $\mathbf{N}^{\pm} = \pm\mathbf{k}$. Their Taylor expansions yield

$$\mathbf{P}^+\mathbf{N}^+ + \mathbf{P}^-\mathbf{N}^- = \epsilon \mathbf{P}_0'\mathbf{k} + o(\epsilon) \quad \text{and} \quad \mathbf{P}^+\mathbf{N}^+ \quad \mathbf{P}^-\mathbf{N}^- = 2\mathbf{P}_0\mathbf{k} + o(\epsilon). \tag{71}$$

On the left hand sides we use (12) together with the estimates

$$(\mathbf{F}^*\mathbf{N})^{\pm} = \pm(\mathbf{F}^*)^{\pm}\mathbf{k} = \pm\mathbf{F}_0^*\mathbf{k} + (\epsilon/2)(\mathbf{F}^*)_0'\mathbf{k} + o(\epsilon) \tag{72}$$

and

$$\alpha^{\pm} = \alpha_0 \pm (\epsilon/2)\alpha_0' + o(\epsilon), \tag{73}$$

where

$$\alpha_0' = \alpha_0^{-1}\mathbf{F}_0^*\mathbf{k} \cdot (\mathbf{F}^*)_0'\mathbf{k}, \tag{74}$$

which follows on differentiation of $\alpha = |\mathbf{F}^*\mathbf{k}|$. After some algebra we obtain

$$\mathbf{P}^+\mathbf{N}^+ + \mathbf{P}^-\mathbf{N}^- = \mathbf{p}_a^+ + \mathbf{p}_a^- + \epsilon\mu_0\alpha_0^{-2}M_0\{[M_0' \quad (\alpha_0'/\alpha_0)M_0] \times \mathbf{F}_0^*\mathbf{k} + \tfrac{1}{2}M_0(\mathbf{F}^*)_0'\mathbf{k}\} + o(\epsilon) \tag{75}$$

and

$$\mathbf{P}^+\mathbf{N}^+ \quad \mathbf{P}^-\mathbf{N}^- = \mathbf{p}_a^+ \quad \mathbf{p}_a^- + \mu_0\alpha_0^{-2}M_0^2\mathbf{F}_0^*\mathbf{k} + O(\epsilon), \tag{76}$$

where $\mathbf{p}_a^{\pm}$ are the applied tractions at the lateral surfaces and $M = \mathbf{M} \cdot \mathbf{k}$. The role of the latter suggests the decomposition

$$\mathbf{M} = \mathbf{1}\ \mathbf{M} + M\mathbf{k}, \tag{77}$$

which yields

$$Div\ \mathbf{M} = Div_{\parallel}(\mathbf{1}\ \mathbf{M}) + M'. \tag{78}$$

It follows from (71) and (75) that (62) yields a well defined differential equation in the limit of small ϵ only if $\mathbf{P}_0'\mathbf{k}$ remains bounded. Further, (63) implies that the deformation gradient and magnetization are bounded on Ω only if $\mathbf{P}_0$ is bounded. From (75) and (76) it is therefore necessary that

$$\mathbf{p}_a^+ + \mathbf{p}_a^- = \epsilon\mathbf{p} + o(\epsilon) \quad \text{and} \quad \mathbf{p}_a^+ \quad \mathbf{p}_a^- = 2\mathbf{q} + o(1), \tag{79}$$

where $\mathbf{p}$ and $\mathbf{q}$ are of order unity in magnitude. It follows that, to leading order in ϵ,

$$\mathbf{P}_0'\mathbf{k} = \mathbf{p} + \mu_0\alpha_0^{-2}M_0\{[M_0' \quad (\alpha_0'/\alpha_0)M_0]\mathbf{F}_0^*\mathbf{k} + \tfrac{1}{2}M_0(\mathbf{F}^*)_0'\mathbf{k}\}$$
$$\text{and} \quad \mathbf{P}_0\mathbf{k} = \mathbf{q} + \tfrac{1}{2}\mu_0\alpha_0^{-2}M_0^2\mathbf{F}_0^*\mathbf{k}. \tag{80}$$

3.2. Estimate of the self field

Before proceeding we obtain an estimate of the leading order self field potential (32). An elementary calculation based on (77) and (78) gives

$$4\pi\varphi_s(\mathbf{y},t) = \epsilon\left\{\int_{\partial\Omega} \frac{\mathbf{1}\ \mathbf{M}_0 \cdot \boldsymbol{\nu}}{|\mathbf{y}\ \ \mathbf{r}|}\,dS \quad \int_\Omega \frac{[Div_{\parallel}(\mathbf{1}\ \mathbf{M}_0) + M_0']}{|\mathbf{y}\ \ \mathbf{r}|}\,dA\right\} + \int_{\partial\kappa^+} \frac{M^+}{|\mathbf{y}\ \ \boldsymbol{\chi}^+|}\,dA \quad \int_{\partial\kappa} \frac{M^-}{|\mathbf{y}\ \ \boldsymbol{\chi}^-|}\,dA + o(\epsilon), \tag{81}$$

where the superscripts $\pm$ identify the values of functions at the upper and lower lateral surfaces $\partial\kappa^{\pm} = \Omega \times \{\pm\epsilon/2\}$ and $\boldsymbol{\nu} \in \Omega'$ is the unit normal exterior to Ω. This is valid provided that $\mathbf{y} \neq \mathbf{r}(\mathbf{u},t)$ for any $\mathbf{u} \in \overline{\Omega}$. To estimate the associated integrals we compute $|\mathbf{v}|' = |\mathbf{v}|^{-1}\mathbf{v} \cdot \mathbf{v}'$, where $\mathbf{v} = \mathbf{y}\ \ \boldsymbol{\chi}(\mathbf{x},t)$ and the derivative is with respect to ς at fixed $\mathbf{y}$. Accordingly, $\mathbf{v}' = \ \mathbf{F}\mathbf{k}$, and (64) gives

$$|\mathbf{y}\ \ \boldsymbol{\chi}|_0' = \ \frac{(\mathbf{y}\ \ \mathbf{r})}{|\mathbf{y}\ \ \mathbf{r}|} \cdot \mathbf{d}. \tag{82}$$

For $\mathbf{y} \neq \mathbf{r}$ this yields

$$\frac{1}{|\mathbf{y}\ \ \boldsymbol{\chi}|^{\pm}} = \frac{1}{|\mathbf{y}\ \ \mathbf{r}|}\left\{1 \pm \frac{\epsilon}{2}\frac{(\mathbf{y}\ \ \mathbf{r})}{|\mathbf{y}\ \ \mathbf{r}|^2} \cdot \mathbf{d}\right\} + o(\epsilon), \tag{83}$$

which, when combined with

$$M^{\pm} = M_0 \pm (\epsilon/2)M_0' + o(\epsilon), \tag{84}$$

results in

$$4\pi\varphi_s(\mathbf{y},t)/\epsilon = \int_{\partial\Omega} \frac{\mathbf{1}\ \mathbf{M}_0 \cdot \boldsymbol{\nu}}{|\mathbf{y}\ \ \mathbf{r}|}\,dS + \int_\Omega \left[\frac{M_0}{|\mathbf{y}\ \ \mathbf{r}|^2}(\mathbf{y}\ \ \mathbf{r}) \cdot \mathbf{d} \quad \frac{Div_{\parallel}(\mathbf{1}\ \mathbf{M}_0)}{|\mathbf{y}\ \ \mathbf{r}|}\right] dA + o(\epsilon)/\epsilon, \tag{85}$$

provided that (83) is uniformly valid over the domain. This limitation effectively restricts the use of (85) to points $\mathbf{y}$ whose distances from the membrane are of order unity compared to ϵ; that is, to points in space whose minimum distances from the deforming membrane surface are large compared to membrane thickness. Accordingly, it may not be used to describe the self field in the interior of the material.

To characterize the magnetic state inside the film, we estimate (32) at an interior point $\overline{\mathbf{x}} \in \kappa$. For points $\mathbf{x}$ near $\overline{\mathbf{x}}$, the presumed differentiability of the deformation implies that $|\overline{\mathbf{y}}\ \ \boldsymbol{\chi}(\mathbf{x},t)| = O(|\boldsymbol{\xi}|)$, where $\boldsymbol{\xi} = \overline{\mathbf{x}}\ \ \mathbf{x}$ and $\overline{\mathbf{y}} = \boldsymbol{\chi}(\overline{\mathbf{x}},t)$. The self field is obtained by computing the gradient of φ_s with respect to $\mathbf{y}$ and evaluating the result at $\overline{\mathbf{y}}$; thus, for $\overline{\mathbf{x}} \notin \partial\kappa$,

$$4\pi\mathbf{h}_s(\overline{\mathbf{y}}) = \int_{\partial\kappa} \frac{(\mathbf{M} \cdot \mathbf{N})\mathbf{u}}{|\overline{\mathbf{y}}\ \ \boldsymbol{\chi}(\mathbf{x})|^2}\,dA \quad \int_\kappa \frac{(Div\ \mathbf{M})\mathbf{u}}{|\overline{\mathbf{y}}\ \ \boldsymbol{\chi}(\mathbf{x})|^2}\,dV,$$
$$\text{where } \mathbf{u} = (\overline{\mathbf{y}}\ \ \boldsymbol{\chi}(\mathbf{x}))/|\overline{\mathbf{y}}\ \ \boldsymbol{\chi}(\mathbf{x})|, \tag{86}$$

in which t has been suppressed. The singularity is of order $|\xi|^2$, which is integrable in κ. Therefore the volume integral makes a contribution of order ϵ. The boundary integral includes a contribution from the surface $\partial\Omega\times(-\epsilon/2,\epsilon/2)$, on which $|\overline{\mathbf{y}}-\boldsymbol{\chi}(\mathbf{x})|$ is strictly bounded away from zero for any ϵ. Accordingly, this too contributes at order ϵ, leaving

$$4\pi\mathbf{h}_s(\overline{\mathbf{y}})=\int_{\partial\kappa^+\cup\partial\kappa}\frac{(\mathbf{M}\cdot\mathbf{N})\mathbf{u}}{|\overline{\mathbf{y}}-\boldsymbol{\chi}(\mathbf{x})|^2}\,dA+O(\epsilon), \tag{87}$$

in which $\mathbf{M}\cdot\mathbf{N}=\pm M^{\pm}$ on $\partial\kappa^{\pm}$, respectively. Thus,

$$\left|\int_{\partial\kappa^+\cup\partial\kappa}\frac{(\mathbf{M}\cdot\mathbf{N})\mathbf{u}}{|\overline{\mathbf{y}}-\boldsymbol{\chi}(\mathbf{x})|^2}\,dA\right|\le\int_{\partial\kappa^+\cup\partial\kappa}\frac{|M^{\pm}|}{|\overline{\mathbf{y}}-\boldsymbol{\chi}(\mathbf{x})|^2}\,dA$$
$$\le\max_{\partial\kappa^+\cup\partial\kappa}|M^{\pm}|\int_{\partial\kappa^+\cup\partial\kappa}\frac{1}{|\overline{\mathbf{y}}-\boldsymbol{\chi}(\mathbf{x})|^2}\,dA. \tag{88}$$

The integrand in the final integral is dominated by its asymptotic behavior near $\overline{\mathbf{x}}$; i.e., by $|\xi|^{-2}$. For small thickness, the integral may then be shown to be $O(|\ln\epsilon|)$ in magnitude. In view of (84), the upper bound remains finite in the limit only if $\max_{\Omega}|M_0|=0$, in which case it is of order $|\epsilon\ln\epsilon|$. This guarantees that $|\mathbf{h}_s(\overline{\mathbf{y}})|$ is finite and vanishes with ϵ. In particular, then,

$$\mathbf{h}_s\quad\text{vanishes on}\quad\Omega,\quad\text{at leading order.} \tag{89}$$

The alternative ($M_0\neq 0$) yields an upper bound of order $|\ln\epsilon|$, which allows the self field to grow without bound as thickness tends to zero. In this case the magnetostatic energy, and therefore the potential energy, may become unbounded. However, this alternative does not *require* the self field to become unbounded, and so our analysis, while suggestive, is not conclusive. In other words, we have only shown that the constraint:

$$M_0=0\quad\text{on}\quad\Omega \tag{90}$$

is sufficient for (89) and for boundedness of the magnetostatic energy. Using (64) and (77), we then derive

$$\mathbf{m}_0\in T_\omega\quad\text{on}\quad\omega,\quad\text{at every}\quad\mathbf{u}\in\Omega. \tag{91}$$

To explore this issue further, consider the part of the potential energy involving magnetization. This is (cf. (35), (36) and (38))

$$E_{mag}=\int_\kappa[W-\frac{1}{2}(\mathbf{h}+\mathbf{h}_a)\cdot\mathbf{m}]\,dV \tag{92}$$

in which $\mathbf{y}$ and $\mathbf{F}$ are fixed, and reduces to

$$E_{mag}=\int_\kappa(W-\mathbf{h}_a\cdot\mathbf{m})\,dV \tag{93}$$

if the self field is negligible; i.e., if (91) holds. Here the magnetization is obtained by solving (27) in which the self field is suppressed, so that E_{mag} is controlled entirely by the deformation. This effectively eliminates the magnetization as an independent variable. In the work of Gioia and James [8] on non deforming films it is proved that minimizers of (92) furnish energies that converge to (93) as film thickness tends to zero. It was also proved that optimal states of magnetization *necessarily* satisfy (91) and that the residual self field vanishes, in accordance with (89) (see also [9]). Further, in [8] it is shown that there is no residual magnetostatic equation to leading order; indeed, the solution (26) to (25) has already been used in the course of obtaining (91) and therefore plays no further role. These results imply that (89) and (91) characterize optimal states of magnetization in a sufficiently thin film, at any fixed deformation. In particular, the magnetostatic energy is negligible at leading order. The Euler equation for the deformation that emerges from this leading order approximation is given by (11) [9], but with *grad* $\mathbf{h}$ replaced by *grad* $\mathbf{h}_a$. This follows from the fact that the variational derivative of $\mathbf{h}_a$, identified by a superposed dot, is purely convective; i.e., $\dot{\mathbf{h}}_a=(grad\,\mathbf{h}_a)\dot{\mathbf{y}}$, if the applied field is a stationary function of $\mathbf{y}$. The claim then follows from (16), which is equivalent to the symmetry of *grad* $\mathbf{h}_a$. Strictly, these results are known to be necessary only for optimal (energy minimizing) states of magnetization and so may not apply to dynamical states. However, in this work we use dynamics solely to facilitate the computation of equilibria. We do not model actual dynamic interactions. Accordingly, we restrict attention to states of magnetization that are energetically optimal at any deformation, equilibrated or otherwise.

Eq. (90) affords the important simplifications:

$$\mathbf{P}_0'\mathbf{k}=\mathbf{p}\quad\text{and}\quad\mathbf{P}_0\mathbf{k}=\mathbf{q}. \tag{94}$$

For points remote from the deforming film (85) is applicable and simplifies, by virtue of (90), to

$$4\pi\varphi_s(\mathbf{y},t)/\epsilon=\int_\Omega\mathbf{1}\,\mathbf{M}_0\cdot\nabla\left(\frac{1}{|\mathbf{y}-\mathbf{r}|}\right)dA+o(\epsilon)/\epsilon, \tag{95}$$

where ∇ is the two dimensional gradient with respect to $\mathbf{u}\in\Omega$ and Green's theorem has been used to combine terms. Proceeding as in the calculation leading to (85), we put $\mathbf{v}(\mathbf{u},t)=\mathbf{y}-\mathbf{r}(\mathbf{u},t)$ and use (65) to derive

$$d(|\mathbf{v}|^{-1})=-|\mathbf{v}|^{-3}\mathbf{v}\cdot d\mathbf{v},\quad\text{where}\quad d\mathbf{v}=-d\mathbf{r}(\mathbf{u})=-\mathbf{f}(d\mathbf{u}), \tag{96}$$

yielding

$$\nabla\left(\frac{1}{|\mathbf{y}-\mathbf{r}|}\right)=|\mathbf{y}-\mathbf{r}|^{-3}\mathbf{f}^t(\mathbf{y}-\mathbf{r}) \tag{97}$$

and

$$4\pi\varphi_s(\mathbf{y},t)/\epsilon=\int_\Omega\frac{\mathbf{f}\mathbf{M}_0}{|\mathbf{y}-\mathbf{r}|^3}\cdot(\mathbf{y}-\mathbf{r})\,dA+o(\epsilon)/\epsilon. \tag{98}$$

A straightforward computation based on (23) generates the scaled self field in the surrounding space:

$$4\pi\mathbf{h}_s(\mathbf{y},t)/\epsilon=\int_\Omega\mathbf{G}(\mathbf{f}\mathbf{M}_0)\,dA(\mathbf{u})+o(\epsilon)/\epsilon,$$
$$\text{where}\quad\mathbf{G}=\frac{3}{|\mathbf{y}-\mathbf{r}|^5}(\mathbf{y}-\mathbf{r})\otimes(\mathbf{y}-\mathbf{r})-\frac{1}{|\mathbf{y}-\mathbf{r}|^3}\mathbf{I} \tag{99}$$

in which $\mathbf{r}(\mathbf{u},\mathbf{t})$ is the membrane position field at time t. Thus, the leading order model generates the dominant part of the self field in the surrounding space (which is of order ϵ) *a posteriori*.

3.3. Loading

Turning now to the loading, suppose the lateral surfaces are subjected to pressures $P^{\pm}$. The applied tractions are

$$\mathbf{p}_a^{\pm}=\mp(P^{\pm})(\mathbf{F}^*)^{\pm}\mathbf{k}, \tag{100}$$

and we assume that

$$P^{\pm}=\epsilon p^{\pm}+o(\epsilon), \tag{101}$$

where $p^{\pm}$ are of order unity. In this case $\mathbf{q}=\mathbf{0}$ and

$$\mathbf{p}=\alpha(\Delta p)\mathbf{n} \tag{102}$$

in (94), where $\Delta p=p^--p^+$ is the net lateral pressure across the membrane.

Invoking (89) and the foregoing thin film approximations, we find that (62) reduces to

$$Div_{\parallel}(\mathbf{P}_0\mathbf{1})+\alpha(\Delta p)\mathbf{n}+\mu_0(grad\,\mathbf{h}_a)_0\mathbf{m}_0=\rho_{\kappa 0}\mathbf{r}, \tag{103}$$

to leading order, where $(grad\,\mathbf{h}_a)_0$ is evaluated using (21) and (22) with $\mathbf{y}$ replaced by $\mathbf{r}$, and

$$\mathbf{P}_0=W_{\mathbf{F}}(\mathbf{F}_0,\mathbf{m}_0)-q_0\mathbf{F}_0^{-t}. \tag{104}$$

This is augmented by the algebraic constraints $(63)_2$ and $(94)_2$. Using (100), (101) and $\mathbf{y}_0=\boldsymbol{\chi}(\mathbf{u},t)=\mathbf{r}$, the *leading order*

constraints are found to be

$$W_{\mathbf{m}}(\mathbf{F}_0,\mathbf{m}_0)=\mu_0\mathbf{h}_a(\mathbf{r}) \quad \text{and} \quad \mathbf{P}_0\mathbf{k}=\mathbf{0}. \tag{105}$$

Together with (64), (67), (77), (90) and (104), these furnish a system for the determination of $\mathbf{r}(\mathbf{u},t)$, $\mathbf{e}(\mathbf{u},t)$, $\mathbf{M}_0(\mathbf{u},t)(=\mathbf{1}\ \mathbf{M}_0)$ and $q_0(\mathbf{u},t)$. In practice we solve the equation obtained on multiplying (103) through by ϵ. This yields the equation of motion for the membrane, which in turn furnishes the leading order approximation to that for a thin sheet. Our preference for (4) over (1) is due the availability of an explicit formula for the gradient of the applied field (cf. (22)). From $(105)_1$ and (64) it is clear that the constraint (91) imposes a restriction, not only on the magnetization, but also on the deformation and director fields $\mathbf{r}$ and $\mathbf{e}$, and thus on the geometry of the film in the presence of an applied field. In particular, this allows the orientation of the tangent plane to the membrane to adjust in response to the applied field.

The literature on magnetoelasticity in thin structures is typically based on an *a priori* constraint of the Kirchoff Love type (i.e., $\mathbf{e}=\mathbf{0}$) on the director field (e.g. [10]). However, in Section 5 we find that solutions deviate substantially from Kirchhoff Love kinematics. Because we have confined attention to states of magnetization that are optimal at any deformation, and thereby eliminated magnetization as an independent variable, it follows by relaxation of constraints that restrictions of the Kirchhoff Love type impede the attainment of minima of the overall potential energy. Indeed, the analysis of [7] indicates that the Kirchhoff Love constraint is generally incompatible with (91). Therefore the present model is optimal relative to formulations in which such constraints are imposed at the outset. Kirchhoff Love kinematics obtain if the effects of deformation and magnetization are uncoupled in the expression for the strain energy function, as in weakly magnetized materials subjected to applied fields of sufficient intensity [7].

Standard mixed traction/position problems consist of the specification of $\mathbf{r}$ and the traction:

$$\boldsymbol{\tau}=\mathbf{P}_0\mathbf{1}\boldsymbol{\nu}, \tag{106}$$

on complementary parts of the boundary curve $\partial\Omega$. Here $\boldsymbol{\tau}$ is the value on $\partial\Omega$ of the exact traction field acting on a part of the cylindrical generating surface of the body where tractions are assigned. In this work we assume position to be prescribed on $\partial\Omega\times[\ \ \epsilon/2,\epsilon/2]$ and thus assign $\mathbf{r}$ everywhere on $\partial\Omega$.

3.4. Solvability of the constraints

We demonstrate the solvability of the constraints $(105)_{1,2}$ for $\mathbf{M}$ and $\mathbf{e}$ at a given deformation $\mathbf{r}(\mathbf{u},t)$ of Ω. To ease the notation, here and henceforth the subscript 0 is suppressed on the understanding that all fields discussed are the restrictions to Ω of three dimensional fields identified by the same symbol. We impose (90) at the outset, and thus find it more convenient to work with a formulation based on the use of $\mathbf{F}$ and $\mathbf{M}$, rather than $\mathbf{F}$ and $\mathbf{m}$, as independent variables. To this end we invoke bulk incompressibility and use (29) to define the function:

$$\tilde{W}(\mathbf{F},\mathbf{M})=W(\mathbf{F},\mathbf{F}\mathbf{M}) \quad \text{for} \quad \mathbf{M}\in\Omega'. \tag{107}$$

Consider a one parameter family of magnetizations $\mathbf{M}(u)\in\Omega'$. Using a superposed dot to denote the derivative with respect to the parameter, we derive $\tilde{W}_{\mathbf{M}}\cdot\dot{\mathbf{M}}=W_{\mathbf{m}}\cdot\mathbf{F}\dot{\mathbf{M}}$ at fixed $\mathbf{F}$, and therefore

$$[\tilde{W}_{\mathbf{M}} \quad \mathbf{F}^t(W_{\mathbf{m}})]\cdot\dot{\mathbf{M}}=0 \quad \text{for all} \quad \dot{\mathbf{M}}\in\Omega', \tag{108}$$

wherein $\tilde{W}_{\mathbf{M}}\in\Omega'$. It follows that $\tilde{W}_{\mathbf{M}}=\mathbf{1}\mathbf{F}^t(W_{\mathbf{m}})$, where $\mathbf{1}\mathbf{F}^t=\mathbf{f}^t$ by virtue of (64); Eq. (108) then implies that

$$\tilde{W}_{\mathbf{M}}=\mu_0\mathbf{f}^t\mathbf{h}_a(\mathbf{r}). \tag{109}$$

We regard this as an equation for $\mathbf{M}$ in which $\mathbf{r}$, $\mathbf{f}$ and $\mathbf{e}$ (hence $\mathbf{F}$) are assigned. To investigate its solvability we compute another derivative, again at fixed $\mathbf{F}$, obtaining

$$(\tilde{W}_{\mathbf{MM}})\dot{\mathbf{M}}=\mathbf{f}^t(W_{\mathbf{mm}})\dot{\mathbf{m}}=[\mathbf{f}^t(W_{\mathbf{mm}})\mathbf{f}]\dot{\mathbf{M}}. \tag{110}$$

Therefore,

$$\dot{\mathbf{M}}\cdot(\tilde{W}_{\mathbf{MM}})\dot{\mathbf{M}}=\mathbf{f}\dot{\mathbf{M}}\cdot(W_{\mathbf{mm}})\mathbf{f}\dot{\mathbf{M}}, \tag{111}$$

which is positive for all non zero $\dot{\mathbf{M}}$ by virtue of $(41)_2$. Accordingly, $\tilde{W}_{\mathbf{MM}}$ is positive definite and $\tilde{W}(\mathbf{F},\cdot)$ is strictly convex. Eq. (109) therefore possesses a unique solution $\hat{\mathbf{M}}$ which minimizes $\tilde{W}$ at fixed $\mathbf{F}$. This in turn determines the magnetization $\mathbf{m}=\mathbf{f}\hat{\mathbf{M}}$, which furnishes the unique solution to

$$W_{\mathbf{m}}=\mu_0\mathbf{h}_a(\mathbf{r}). \tag{112}$$

Next, we fix $\mathbf{f}$ and define

$$G(\mathbf{e},\mathbf{m})=W(\mathbf{f}+\mathbf{d}(\mathbf{f},\mathbf{e})\otimes\mathbf{k},\mathbf{m}), \tag{113}$$

where $\mathbf{d}(\mathbf{f},\mathbf{e})$ is the function defined by (67), in which α and $\mathbf{n}$ are determined by $\mathbf{f}$ via (68) and (70). Consider one parameter families $\mathbf{e}(u)$ and $\mathbf{m}(u)$. The former induces the one parameter family $\mathbf{F}(u)$ of deformation gradients with derivative $\dot{\mathbf{F}}=\mathbf{f}\dot{\mathbf{e}}\otimes\mathbf{k}$ (cf. (64) and (67)). Accordingly,

$$\dot{G}=\dot{\mathbf{e}}\cdot\mathbf{f}^t(W_{\mathbf{F}})\mathbf{k}+\dot{\mathbf{m}}\cdot W_{\mathbf{m}},$$
$$\text{yielding} \quad G_{\mathbf{e}}=\mathbf{f}^t(W_{\mathbf{F}})\mathbf{k} \quad \text{and} \quad G_{\mathbf{m}}=W_{\mathbf{m}}. \tag{114}$$

Using (104) and the invertibility of $\mathbf{F}^t$, we find the constraint $(105)_2$ to be equivalent to

$$G_{\mathbf{e}}=\mathbf{0} \quad \text{and} \quad q=\mathbf{d}\cdot(W_{\mathbf{F}})\mathbf{k}. \tag{115}$$

To address the first of these equations, we keep $\mathbf{f}$ fixed and compute:

$$(G_{\mathbf{e}})^{\cdot}=\mathbf{f}^t\{W_{\mathbf{FF}}[\mathbf{f}\dot{\mathbf{e}}\otimes\mathbf{k}]+(W_{\mathbf{Fm}})\dot{\mathbf{m}}\}\mathbf{k}. \tag{116}$$

Here we regard $\mathbf{m}(u)$ as the magnetization induced by $\mathbf{e}(u)$ via (112); that is, we use the unique solution $\mathbf{M}=\hat{\mathbf{M}}(\mathbf{e})$ to (109), associated with fixed $\mathbf{r}$ and $\mathbf{f}$, to generate $\mathbf{m}(u)=\mathbf{f}\hat{\mathbf{M}}(\mathbf{e}(u))$. This satisfies (112) identically for all $\mathbf{e}(u)$ with u in some open interval. It follows that

$$\dot{\mathbf{m}}= \quad (W_{\mathbf{mm}})^{-1}(W_{\mathbf{mF}})(\mathbf{f}\dot{\mathbf{e}}\otimes\mathbf{k}), \tag{117}$$

so that (116) reduces to

$$(G_{\mathbf{e}})^{\cdot}=\mathbf{f}^t\{\mathbf{A}(\mathbf{k})\}(\mathbf{f}\dot{\mathbf{e}}), \tag{118}$$

where $\mathbf{A}(\cdot)$ is defined by (42).

With these results in hand, we define a function $\Gamma(\mathbf{e})$ by

$$\Gamma(\mathbf{e})=G(\mathbf{e},\mathbf{f}\hat{\mathbf{M}}(\mathbf{e})) \quad \mu_0\mathbf{h}_a(\mathbf{r})\cdot\mathbf{f}\hat{\mathbf{M}}(\mathbf{e}), \tag{119}$$

at the same $\mathbf{r}$ and $\mathbf{f}$. Inserting $\mathbf{e}(u)$ and evaluating the derivative, we find from (112) and $(114)_2$ that

$$\dot{\Gamma}=G_{\mathbf{e}}\cdot\dot{\mathbf{e}} \tag{120}$$

for all u in some open interval. Then,

$$\Gamma=(G_{\mathbf{e}})^{\cdot}\cdot\dot{\mathbf{e}}+G_{\mathbf{e}}\cdot\mathbf{e}. \tag{121}$$

The domain of $\Gamma(\cdot)$ is the linear space Ω', a convex set. If $\mathbf{e}_{1,2}$ belong to this domain, then so do all points on the straight line path

$$\mathbf{e}(u)=u\mathbf{e}_2+(1 \quad u)\mathbf{e}_1; \quad u\in(0,1), \tag{122}$$

on which (121) reduces to

$$\Gamma=\mathbf{f}\dot{\mathbf{e}}\cdot\{\mathbf{A}(\mathbf{k})\}(\mathbf{f}\dot{\mathbf{e}}); \quad \dot{\mathbf{e}}=\mathbf{e}_2 \quad \mathbf{e}_1\neq\mathbf{0}. \tag{123}$$

Setting $\mathbf{a}=\mathbf{f}\dot{\mathbf{e}}\in T_\omega$ and $\mathbf{b}=\mathbf{k}$, we find that (43) is satisfied because $\mathbf{F}^*\mathbf{k}=\alpha\mathbf{n}$ is orthogonal to T_ω (cf. (68)). Accordingly, the strong ellipticity inequality $(41)_1$ is applicable and implies that $\Gamma>0$. Integration of this result over $(0,u)$ and then again over $(0,1)$

yields the conclusion that $\Gamma(\mathbf{e})$ is strictly convex; i.e.,

$$\Gamma(\mathbf{e}_2) \quad \Gamma(\mathbf{e}_1) > \Gamma_{\mathbf{e}}(\mathbf{e}_1)\cdot(\mathbf{e}_2 \quad \mathbf{e}_1) \tag{124}$$

for all unequal pairs $\mathbf{e}_{1,2}$, wherein $\Gamma_{\mathbf{e}} = G_{\mathbf{e}}$ by virtue of (120). Because strictly convex functions possess unique stationary points, we conclude that $(115)_1$ has a unique solution $\mathbf{e}^*$. In particular, this solution satisfies $\Gamma(\mathbf{e}) > \Gamma(\mathbf{e}^*)$ for all $\mathbf{e} \neq \mathbf{e}^*$ and therefore furnishes the unique minimizer of $\Gamma(\mathbf{e})$. With this solution in hand, the unique magnetization field associated with a given deformation $\mathbf{r}(\mathbf{u},t)$, and attendant gradient $\mathbf{f}$, is given by $\mathbf{m} = \mathbf{f}\hat{\mathbf{M}}(\mathbf{e}^*)$.

3.5. Lyapunov functions

We have shown that the constraints (109) and $(115)_1$ possess unique solutions $\mathbf{e}$ and $\mathbf{M}$ at fixed $\mathbf{r}$ and $\mathbf{f}$. To obtain them, use may be made of the Newton Raphson method, for example. The convexity conditions established in the foregoing ensure that the associated iterates converge to a unique solution. Alternatively, we may embed (109) and $(115)_1$ into the artificial dynamical problems:

$$m\ddot{\mathbf{M}} + c\dot{\mathbf{M}} + \tilde{W}_{\mathbf{M}} = \mu_0 \mathbf{f}^t \mathbf{h}_a(\mathbf{r}) \quad \text{and} \quad m\ddot{\mathbf{e}} + c\dot{\mathbf{e}} + G_{\mathbf{e}} = \mathbf{0}, \tag{125}$$

respectively, in which m and c are positive constants and the superposed dots in the two equations now identify derivatives with respect to time like parameters $\tau_{1,2}$, respectively. Equilibria of this system are precisely the unique solutions to (109) and $(115)_1$. Further, solutions to this system satisfy the energy balances:

$$\frac{d}{d\tau_1}\left(\frac{1}{2}m|\dot{\mathbf{M}}|^2 + \tilde{W}\right) = \quad c|\dot{\mathbf{M}}|^2 \quad \text{and} \quad \frac{d}{d\tau_2}\left(\frac{1}{2}m|\dot{\mathbf{e}}|^2 + \Gamma\right) = \quad c|\dot{\mathbf{e}}|^2. \tag{126}$$

Standard theory for ordinary differential equations then ensures the existence of trajectories of $(125)_{1,2}$ for arbitrary initial data on which

$$L_1 = \tfrac{1}{2}m|\dot{\mathbf{M}}|^2 + \tilde{W} \quad \text{and} \quad L_2 = \tfrac{1}{2}m|\dot{\mathbf{e}}|^2 + \Gamma \tag{127}$$

are strictly decreasing. Our results concerning the minimizing properties of equilibria then imply that $L_{1,2}$ furnish Lyapunov functions for $(125)_{1,2}$, respectively. All trajectories tend asympto tically to solutions of the constraints (109) and $(115)_1$, and these are stable equilibria of the dynamical system [21]. The imple mentation of these results is discussed in Section 4.

Finally, we use the energy balance (37) to construct a Lyapu nov function for the motion $\mathbf{r}(\mathbf{u},t)$. To this end we observe, using (34) (36), (38) and (39) that

$$K = \epsilon K_M + o(\epsilon), \quad L = \epsilon L_M + o(\epsilon) \quad \text{and} \quad E = \epsilon E_M + o(\epsilon), \tag{128}$$

where

$$K_M = \frac{1}{2}\int_\Omega \rho_\kappa |\dot{\mathbf{r}}|^2 \, dA, \quad L_M = \int^V p^-(v)\, dv \quad p^+ V$$
$$\text{and} \quad E_M = \int_\Omega W(\mathbf{F},\mathbf{m})\, dA \quad \mu_0 \int_\Omega \mathbf{h}_a(\mathbf{r})\cdot\mathbf{m}\, dA \quad L_M, \tag{129}$$

respectively, are the leading order (membrane) approximations to the kinetic energy, pressure potential, and potential energy, in which

$$V = \frac{1}{3}\int_\Omega \alpha \mathbf{n}\cdot\mathbf{r}\, dA \tag{130}$$

is the volume of the compressible gas contained by the mem brane. From the leading order equation of motion (103), we obtain

$$\dot{K}_M = \int_\Omega \dot{\mathbf{r}}\cdot[Div_\parallel(\mathbf{P1}) + \alpha(\Delta p)\mathbf{n} + \mu_0(grad\ \mathbf{h}_a)\mathbf{m}]\, dA. \tag{131}$$

Using [9]

$$\dot{L}_M = \int_\Omega \alpha(\Delta p)\mathbf{n}\cdot\dot{\mathbf{r}}\, dA \tag{132}$$

this is reduced to

$$\dot{K}_M = \dot{L}_M + \mu_0 \int_\Omega \mathbf{m}\cdot\dot{\mathbf{h}}_a\, dA + \int_{\partial\Omega} \mathbf{P1}\boldsymbol{\nu}\cdot\dot{\mathbf{r}}\, dS \quad \int_\Omega \mathbf{P1}\cdot\dot{\mathbf{f}}\, dA, \tag{133}$$

where we have used $\dot{\mathbf{h}}_a = (grad\ \mathbf{h}_a)\dot{\mathbf{r}}$ for stationary applied fields, together with the symmetry of $grad\ \mathbf{h}_a$. In this work we assume $\mathbf{r}$ to be fixed on $\partial\Omega$ and accordingly suppress the integral over $\partial\Omega$. We now use $(105)_1$ and combine the result with $(129)_3$ to derive

$$\frac{d}{dt}(K_M + E_M) = \int_\Omega (W_{\mathbf{F}}\cdot\dot{\mathbf{F}} \quad \mathbf{P1}\cdot\dot{\mathbf{f}})\, dA. \tag{134}$$

Using (104) with the constraint of bulk incompressibility in the form $\mathbf{F}^{-t}\cdot\dot{\mathbf{F}} = 0$, together with (59) and (64), we find that

$$W_{\mathbf{F}}\cdot\dot{\mathbf{F}} = \mathbf{P}\cdot\dot{\mathbf{F}} = \mathbf{P1}\cdot\dot{\mathbf{f}} + \mathbf{Pk}\cdot\dot{\mathbf{d}} \tag{135}$$

and thereby reduce (134) to

$$\frac{d}{dt}(K_M + E_M) = \int_\Omega \mathbf{Pk}\cdot\dot{\mathbf{d}}\, dA, \tag{136}$$

which vanishes by virtue of (105). Thus the leading order model yields the conservation law $(d/dt)(K_M + E_M) = 0$, which is replaced, in the presence of dissipation, by the imbalance $(d/dt)(K_M + E_M) \leq 0$. This observation suggests that a dissipative *numer ical scheme* may be based on a discretization of the *artificial* dynamical equation:

$$Div_\parallel(\mathbf{P1}) + \alpha(\Delta p)\mathbf{n} + \mu_0(grad\ \mathbf{h}_a)\mathbf{m} = \rho_\kappa \mathbf{r} + c\dot{\mathbf{r}}, \tag{137}$$

where c is a suitable constant. It is straightforward to show that if this equation is used in place of (103), then the leading order energy balance is replaced by

$$\frac{d}{dt}(K_M + E_M) = \quad c\int_\Omega |\dot{\mathbf{r}}|^2\, dA. \tag{138}$$

Our earlier observation that stable equilibria minimize E implies that E_M is minimized, to leading order in thickness. Indeed, it is easily verified that (112) and the static specialization of (103) furnish the Euler Lagrange equations for E_M. Consequently, $K_M + E_M$ decays on trajectories of (137), provided that $c > 0$, and achieves a strict minimum at a stable equilibrium. It therefore yields a Lyapunov function for (137), whose equilibria coincide with those of (103). This conclusion applies strictly only to a finite dimensional projection of the problem associated with a spatial discretization of the equations on Ω. It also presumes that equilibria are minimizers of E_M. Here, however, we have only imposed necessary conditions for a minimum of the energy. In particular, in the purely mechanical specialization of the theory it is known that these conditions are insufficient to preclude compressive stresses in equilibrium, which violate the Legendre Hadamard necessary condition for minimizers of E_M [25]. In such circumstances the existence of minimizers may be restored by replacing the membrane energy with a suitable *relaxation* [25 28] which excludes compressive stress *a priori* via the mechanism of fine scale wrinkling. This is the subject of *tension field theory* [29]. In this work we apply the theory to problems that do not exhibit wrinkling and therefore do not require the explicit relaxation.

We emphasize the fact that (137) does not describe the actual dynamics of the membrane. Rather, it is used here solely to expedite the computation of equilibria by embedding the equili brium problem into an artificial (finite dimensional) dynamical system whose equilibria coincide with those of the physical problem. As such, it furnishes a convenient regularization of the equations. The strictly dissipative nature of this system is a feature shared by actual equations of motion that account for

dissipation through *constitutive* equations rather than through modification of the equation of motion. However, (137) proves more convenient for the purpose of generating *equilibria* because it allows the discrete equations associated with the temporal evolution to be decoupled, affording a more efficient solution procedure. This is discussed in the next section.

4. Finite-difference scheme

Equation (137) is discretized by using a finite difference scheme derived from Green's theorem. The application of this scheme to plane strain problems in non linear elasticity theory is described by Silling [30]. Its adaptation to membrane theory is developed in [26,27]. Here, we summarize the method and describe its extension to magnetoelasticity.

The reference plane Ω is covered by a grid consisting of cells of the kind depicted in Fig. 1. Nodes are labeled using integer superscripts (i,j). Thus, $u_\alpha^{i,j}$ are the referential coordinates of node (i,j), where $u_\alpha = \mathbf{u}\cdot\mathbf{i}_\alpha$; $\alpha = 1,2$. The four regions formed by a node, together with its nearest neighbor nodes, are called *zones*. Zone centered points, identified by open circles in Fig. 1, are labeled using half integer superscripts.

Green's theorem may be stated in the form:

$$\int_D \sigma_{\alpha,\alpha}\, da = e_{\alpha\beta}\int_{\partial D}\sigma_\alpha\, du_\beta, \tag{139}$$

where $\sigma_\alpha(u_1,u_2)$ is a smooth two dimensional vector field, D is an arbitrary simply connected subregion of Ω and commas followed by subscripts identify partial derivatives with respect to the indicated coordinates. To approximate the divergence $\sigma_{\alpha,\alpha}$ at node (i,j) we identify D with the quadrilateral contained within the dashed contour of Fig. 1. The left hand side of (114) is estimated as the nodal value of the integrand multiplied by the area of D; the right hand side as the zone centered values of the integrand on each of the four edges of ∂D multiplied by the appropriate edge length. Thus [26],

$$\begin{aligned}2A^{i,j}(\sigma_{\alpha,\alpha})^{i,j} = e_{\alpha\beta}[&\sigma_\alpha^{i+1/2,j+1/2}(u_\beta^{i,j+1}\quad u_\beta^{i+1,j})\\ &+\sigma_\alpha^{i-1/2,j+1/2}(u_\beta^{i-1,j}\quad u_\beta^{i,j+1})\\ &+\sigma_\alpha^{i-1/2,j-1/2}(u_\beta^{i,j-1}\quad u_\beta^{i-1,j})\\ &+\sigma_\alpha^{i+1/2,j-1/2}(u_\beta^{i+1,j}\quad u_\beta^{i,j-1})],\end{aligned} \tag{140}$$

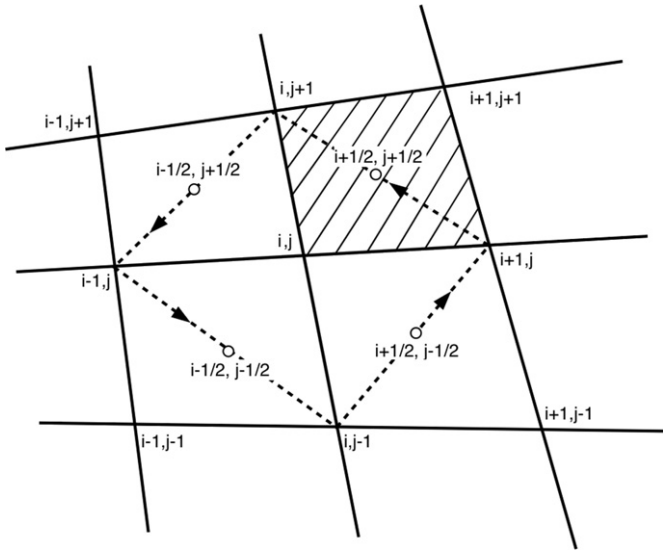

Fig. 1. Finite-difference mesh.

where

$$A^{i,j} = \tfrac{1}{4}[(u_2^{i-1,j}\quad u_2^{i+1,j})(u_1^{i,j+1}\quad u_1^{i,j-1})\quad(u_1^{i-1,j}\quad u_1^{i+1,j})(u_2^{i,j+1}\quad u_2^{i,j-1})] \tag{141}$$

is one half the area of the quadrilateral.

We also have need of gradients of various functions at zone centered points. First, we apply (139) with $\sigma_\alpha = c_\alpha\sigma(u_1,u_2)$, where σ is a smooth scalar field and c_α are arbitrary constants. This yields

$$\int_D \sigma_{,\alpha}\, da = e_{\alpha\beta}\int_{\partial D}\sigma\, du_\beta. \tag{142}$$

We now identify D with the shaded region in the figure. The left hand side is approximated by the product of the shaded area with the integrand, evaluated at the zone centered point, and the four edge contributions to the right hand side are approximated by replacing the integrand in each with the average of the nodal values at the endpoints. This gives [26]

$$\begin{aligned}2A^{i+1/2,j+1/2}(\sigma_{,\alpha}^{i+1/2,j+1/2}) = e_{\alpha\beta}[&(\sigma^{i+1,j+1}\quad \sigma^{i,j})(u_\beta^{i,j+1}\quad u_\beta^{i+1,j})\\ &(\sigma^{i,j+1}\quad \sigma^{i+1,j})(u_\beta^{i+1,j+1}\quad u_\beta^{i,j})],\end{aligned} \tag{143}$$

where

$$\begin{aligned}A^{i+1/2,j+1/2} = \tfrac{1}{2}[&(u_2^{i,j+1}\quad u_2^{i+1,j})(u_1^{i+1,j+1}\quad u_1^{i,j})\quad(u_1^{i,j+1}\quad u_1^{i+1,j})\\ &(u_2^{i+1,j+1}\quad u_2^{i,j})].\end{aligned} \tag{144}$$

The magnetoelastic equilibrium equation is given by (137) in which the right hand side is suppressed. To facilitate its discretization, we exploit the fact that the term $\alpha\mathbf{n}$ associated with the pressure load may be expressed as a divergence on Ω [31]. Thus, $\mathbf{n} = n_k\mathbf{i}_k$, where $\mathbf{i}_3 = \mathbf{k}$,

$$\alpha n_k = \tfrac{1}{2}e_{ijk}e_{\alpha\beta}f_{i\alpha}f_{j\beta} = G_{k\beta,\beta}, \tag{145}$$

and

$$G_{k\beta} = \tfrac{1}{2}e_{ijk}e_{\alpha\beta}f_{i\alpha}r_j \tag{146}$$

in which e_{ijk} and $e_{\alpha\beta}$, respectively, are the three and two dimensional unit alternators ($e_{123} = e_{12} = +1$). This result is useful in the present circumstances because the net lateral pressure on the membrane is uniformly distributed. Thus, the equilibrium equation is equivalent to the system

$$T_{k\alpha,\alpha} = R_k,\quad \text{where}\quad T_{k\alpha} = P_{k\alpha} + (\Delta p)G_{k\alpha}\quad\text{and}\quad R_k = \mu_0 h_{k,i}^{(a)} f_{i\alpha}M_\alpha. \tag{147}$$

Here $P_{k\alpha} = \mathbf{P}\cdot\mathbf{i}_k\otimes\mathbf{i}_\alpha$ are the components of $\mathbf{P1}$, $h_k^{(a)} = \mathbf{i}_k\cdot\mathbf{h}_a$ are the components of the applied field, $f_{k\alpha} = \mathbf{f}\cdot\mathbf{i}_k\otimes\mathbf{i}_\alpha = r_{k,\alpha}$ are the components of the surface deformation gradient, $r_k = \mathbf{i}_k\cdot\mathbf{r}$ are the Cartesian coordinates of a material point on the deformed surface and $M_\alpha = \mathbf{M}\cdot\mathbf{i}_\alpha$ are the magnetization components.

Each of Eqs. (147) is of the form:

$$\sigma_{\alpha,\alpha} = f, \tag{148}$$

where $\sigma_\alpha = T_{k\alpha}$ and $f = R_k$; $k = 1,2,3$. The σ_α, in turn, depend on the magnetization and on the gradients of $\sigma = r_k$ $(k = 1,2,3)$. To solve (148) at node (i,j) we integrate it over the region enclosed by the dashed quadrilateral of Fig. 1 with vertices at the nearest neighbor nodes, obtaining

$$\Sigma^{i,j} = F^{i,j}, \tag{149}$$

where

$$\Sigma^{i,j} = 2A^{i,j}(\sigma_{\alpha,\alpha})^{i,j} \tag{150}$$

and

$$F^{i,j} = 2A^{i,j}f^{i,j}. \tag{151}$$

In (150) the right hand side is evaluated in terms of the zone centered values of σ_α via (140). The latter are determined constitutively by corresponding zone centered values of magnetization together with the gradients $\sigma_{,\alpha}$ which, in turn, are given via (143) by the values of σ at the nodes located at the vertices of the shaded region of Fig. 1. The scheme is seen to require one degree less differentiability than that required by the local differential equations. Discussions of the associated truncation errors are given by Silling [30] and Hermann and Bertholf [32].

To solve Eq. (149) we introduce a regularization based on the artificial dynamical system (cf. (137)):

$$\Sigma^{i,j,n} = m^{i,j}\sigma^{i,j,n} + c^{i,j}\dot{\sigma}^{i,j,n} + F^{i,j,n}, \tag{152}$$

where $m^{i,j} = 2A^{i,j}\rho$ is the nodal mass, $c^{i,j} = 2A^{i,j}c$ is the nodal damping coefficient, n is the time step, and superposed dots refer to derivatives with respect to (artificial) time. This is *not* the discrete form of the actual dynamical equations. Rather, it is an artificial system introduced solely to expedite the computation of equilibria. The basic method, known as *dynamic relaxation* [33], is a powerful tool for generating equilibria in a wide variety of nonlinear problems. It was developed for membrane theory in a purely mechanical setting in [26 28] and extended to coupled thermoelasticity in [31].

We observe that the matrix $G_{k\beta}$ associated with lateral pressure is evaluated at zone centered points (cf. (147) and (150)). However, this involves the deformation r_k (cf. (146)), a nodal variable. The required evaluation is based on the average of the deformations at the four adjacent nodes. Similarly, (147) requires nodal values of $f_{k\alpha}M_\alpha$, which are obtained by averaging values at the four adjacent zone centered points.

In the case of volume dependent pressure loading it is necessary to evaluate the volume enclosed by the deformed membrane and the plane Ω. This is obtained from (130) in which $\alpha\mathbf{n}\cdot\mathbf{r} = \frac{1}{2}e_{ijk}e_{\alpha\beta}f_{i\alpha}f_{j\beta}r_k$. The domain is divided into zones the shaded regions in Fig. 1 and the integral over each is estimated as the zone centered value of the integrand multiplied by the shaded area, given by (144). Similarly, the scaled self field at a given position $\mathbf{y}$ in the surrounding space is obtained by using (99), in which the integral is replaced by the sum of the integrals over the zones. Each of these is approximated by multiplying the value of the integrand at the relevant zone centered point by the shaded area. The integrand is formed from zone centered values of $\mathbf{f}$ and $\mathbf{M}$ and the averaged values of the nodal membrane position $\mathbf{r}$.

The time derivatives in (152) are approximated by the central differences:

$$\dot{\sigma}^n = \frac{1}{2}(\dot{\sigma}^{n+1/2} + \dot{\sigma}^{n-1/2}), \quad \sigma^n = \frac{1}{h}(\dot{\sigma}^{n+1/2} \quad \dot{\sigma}^{n-1/2}),$$
$$\dot{\sigma}^{n-1/2} = \frac{1}{h}(\sigma^n \quad \sigma^{n-1}), \tag{153}$$

where h is the time increment and the node label (i,j) has been suppressed. Substitution into (152) furnishes the explicit, decoupled system:

$$(h^{-1} + c/2)m^{i,j}\dot{\sigma}^{i,j,n+1/2} = (h^{-1} \quad c/2)m^{i,j}\dot{\sigma}^{i,j,n-1/2} + \Sigma^{i,j,n} \quad F^{i,j,n},$$
$$\sigma^{i,j,n+1} = \sigma^{i,j,n} + h\dot{\sigma}^{i,j,n+1/2}, \tag{154}$$

which is used to advance the solution in time node by node. The stress at zone centered points is updated by using (64), (65), (104), in which the reactive constraint pressure q is computed from (67), (68) and $(115)_2$.

The starting procedure is derived from the quiescent initial conditions:

$$\sigma^{i,j,0} = \sigma_0(u_\alpha^{i,j}), \quad \dot{\sigma}^{i,j,0} = 0, \tag{155}$$

where $\sigma_0(u_\alpha)$ is assigned. Thus, from (154) we obtain

$$(2/h)m^{i,j}\dot{\sigma}^{i,j,1/2} = \Sigma^{i,j,0} \quad F^{i,j,0}, \tag{156}$$

in which the right hand side is determined by the function σ_0. The system is non dimensionalized and the solution is advanced to the first t_n such that $\max_{i,j} |\Sigma^{i,j,n} \quad F^{i,j,n}| < \delta$, a suitable tolerance. We remark that because only long time limits of solutions are relevant, temporal accuracy is not an issue. Stability is addressed by using sufficiently small time steps selected on the basis of successive trials based on a sequence of values of h.

A similar temporal discretization is used to update the magnetization and director fields $\mathbf{M}$ and $\mathbf{e}$ at zone centered points. Consistency with the derivation of the Lyapunov functions $L_{1,2}$ of Section 3 requires the use of a staggered scheme in which the predicted position field at time step $n+1$ is fixed while integrating (126). We then start the integration of $(126)_2$ using the value of $\mathbf{e}$ at step n as the initial condition (with the initial value $\dot{\mathbf{e}} = \mathbf{0}$). This calculation proceeds in increments of the time like variable τ_2. We fix the predicted value of $\mathbf{e}$ at the subsequent step and use this value to integrate $(126)_1$ with respect to τ_1, using the value of $\mathbf{M}$ generated by the previous value of $\mathbf{e}$ as the initial condition (with initial value $\dot{\mathbf{M}} = \mathbf{0}$). This continues until convergence is achieved, yielding the magnetization associated with the predicted value of $\mathbf{e}$. The integration with respect to τ_2 then resumes and the cycle is repeated until convergence is achieved, yielding the values of $\mathbf{e}$ and $\mathbf{M}$ associated with the position field at step $n+1$. The process is repeated until the deformation field converges, yielding the final equilibrium position, magnetization and director fields over all nodes and zone centered points. However, numerical experiments indicate that this computationally intensive double staggered scheme is not required in practice. Instead, we find that equilibrium states may be achieved by treating all fields on an equal basis as far as temporal integration is concerned.

The magnetization at step $n=0$ is set to zero. This is the unique solution to (112) if the applied field vanishes. Accordingly, the applied field intensity is first set to a small value and the equilibrium fields are obtained by the foregoing procedure. Successive equilibria are then computed for a sequence of increasing field intensities, using the equilibria associated with each member of the sequence as initial values for the next member.

5. Examples

In this final section we discuss the results of some numerical experiments. All examples pertain to a membrane that is initially square, of side 8 mm and thickness $h = 50 \times 10^{-3}$ mm. The latter is used in place of ϵ in the formula (99) for the self field, which was derived using a scheme in which ϵ is interpreted as (dimensionless) thickness. The mass density is $\rho = 1750\ \mathrm{kg/m^3}$; the free space permeability is $\mu_0 = 4\pi \times 10^{-7}\ \mathrm{N/A^2}$ (Newton per square Ampere) [14]; and the dipole source is centrally located above the plane at $\mathbf{y}_d = (8\ \mathrm{mm})\mathbf{k}$. We find that convergence is achieved in all cases using a regular 33×33 mesh. Material parameters are taken to be those suggested in [34]. Thus, the saturation magnetization is $\overline{M}_s = \mu_0/2$, the shear modulus is $\mu = 1.0 \times 10^6\ \mathrm{N/m^2}$, and the remaining parameters in (56) are $C_{10} = 1.0$, $C_{20} = 0.625$, $C_{11} = 0.0791$, $C_{21} = 0.0$, $C_{01} = \beta/6$ and $C_{02} = \beta/2$, where $\beta = \mu_0\overline{M}_s^2/2$.

Fig. 2 depicts the deformation of the membrane under zero pressure in response to a dipole of strength $D = 160 \times 10^{-6}\ \mathrm{A\,m^2}$ (cf. (20)). The vertical and in plane dimensions are scaled differently to aid in visualization. We have used the data generated by the simulation, together with (69), to verify that the three dimensional principal stretches on the membrane surface are

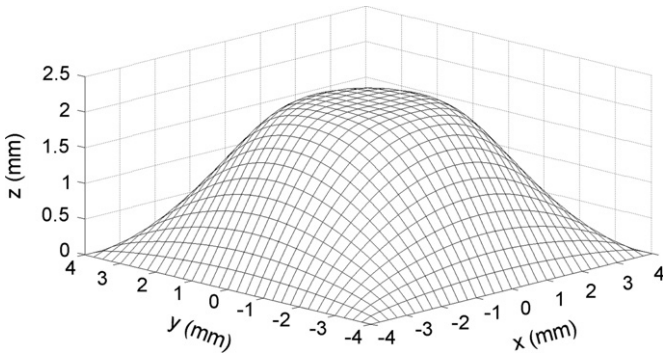

Fig. 2. Deformed membrane at $D \quad 160 \times 10^{6}$ A m^2.

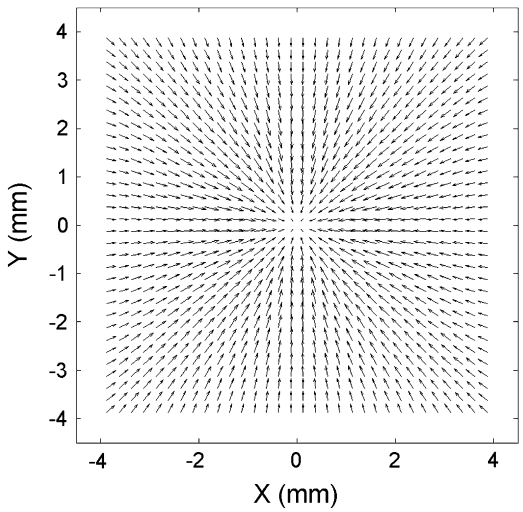

Fig. 3. Referential magnetization at $D \quad 160 \times 10^{6}$ A m^2 on the reference plane.

well within the limits required for the validity of $(41)_2$. The referential in plane magnetization field **M** is shown in Fig. 3.

This field is directed everywhere toward the center of the membrane, where differentiability requires that it diminish to zero in intensity. This and the constraint (91) cause the interac tion with the applied field to weaken near the center, resulting in a deformed surface that is relatively flat under the dipole source.

Fig. 4 shows the variation of the in plane part, **e**, of the director field with respect to position on the reference plane. The defor mation deviates from Kirchhoff Love kinematics wherever this is non zero. This reflects the bias induced by the dipole source at points lying off the dipole axis, causing the director **d** on the deformed surface to tilt relative to the tangent plane as the membrane adjusts to the applied field. The effect diminishes near the corners of the membrane where the field is relatively weak, and near the center where the field lines intersect the membrane orthogonally and the associated bias vanishes; in either case the kinematics revert to the Kirchhoff Love mode. Fig. 5 illustrates the self field generated by the membrane, computed *post facto* using (99), in a plane of symmetry obtained by fixing a reference coordinate at the value zero.

Finally, the effects of pre stretch and pressure are displayed in Fig. 6, in which the height of the deformed surface, at a point on the dipole axis, is plotted against dipole strength. The open circles and crosses correspond to zero applied pressure; the former corresponding to no pre stretch and the latter to a uniform pre stretch of 1.2 induced by an outward displacement of nodes on the boundary; these are subsequently fixed in the course of the simulation. Pre stretch is seen to stiffen the membrane

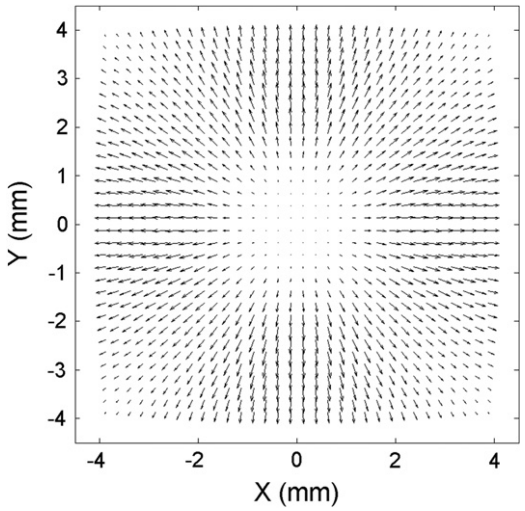

Fig. 4. In-plane part, **e**, of director field, at $D \quad 160 \times 10^{6}$ A m^2.

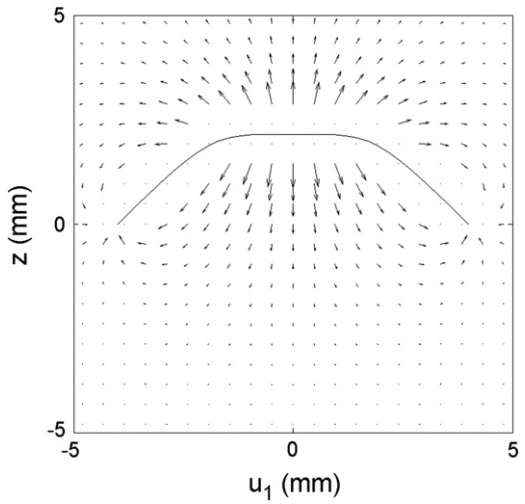

Fig. 5. Self-field in space at $D \quad 160 \times 10^{6}$ A m^2, in the plane defined by $u_2 \quad 0$.

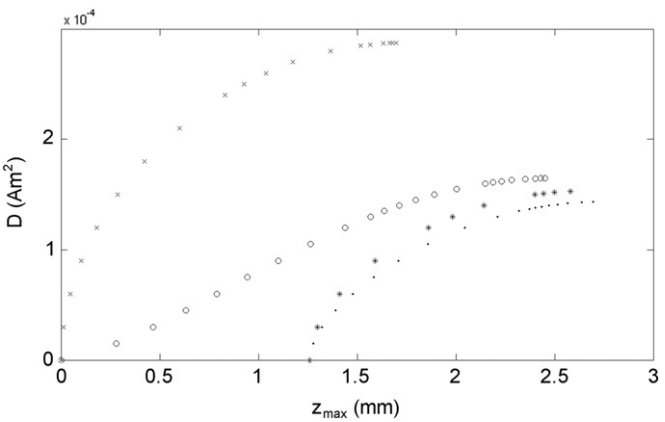

Fig. 6. Membrane displacement under the dipole source, as a function of dipole strength. Effect of pre-stretch indicated by circles (◦) and crosses (×); effect of fixed or volume-dependent pressure is indicated by dots (·) and stars (*), respectively (see text).

dramatically, resulting in a much smaller deflection at any given field strength. The effect of pressure (at no pre stretch) is illustrated by the dotted and starred data, the former correspond ing to a fixed inflation pressure $P = 2.0 \times 10^5$ Pa acting on the

interior of the membrane; the external pressure is assumed to vanish. This is regarded as being supplied by a large reservoir with an opening on the reference plane. The stars correspond to a volume-dependent pressure in which the product of the pressure and the enclosed volume remains constant, as in an ideal gas at fixed temperature. The constant is derived by using (130) to compute the contained volume generated in response to the fixed pressure at zero field strength. As expected, pressure has a significant effect on deformation at small field intensities, but its relative importance diminishes with increasing intensity. Moreover, at any value of field intensity the volume-dependent pressure yields a smaller displacement than that produced by the fixed pressure. The discrepancy increases with field intensity due to the attendant increase in volume, which causes the volume-dependent pressure to be reduced in magnitude. In all cases an upper limit is predicted for the deformation that can be maintained in equilibrium. Such limits are identified by the failure of the dynamic relaxation method to generate equilibria when the field intensity is increased above a critical value. Our results thus establish the existence of a limit-point instability at sufficiently high field intensities. This corroborates the analysis of [35], based on a low-order finite-dimensional projection of the model developed in [7].

Acknowledgments

This work was performed under the auspices of the U.S. Department of Energy by the University of California, Lawrence Livermore National Laboratory under contract DE-AC52-07NA27344. It was conducted during the tenure of a Lawrence Scholarship held by M. Barham from 2008 to 2011 in support of graduate studies at the University of California, Berkeley.

References

[1] A. Dorfmann, R.W. Ogden, Magnetoelastic modeling of elastomers, Euro. J. Mech. A Solids 22 (2003) 497–507.
[2] A. Dorfmann, R.W. Ogden, Nonlinear magnetoelastic deformations of elastomers, Acta Mech. 167 (2004) 13–28.
[3] R. Bustamante, A. Dorfmann, R.W. Ogden, On variational formulations in nonlinear magnetoelastostatics, Math. Mech. Solids 13 (2008) 725–745.
[4] R. Bustamante, A. Dorfmann, R.W. Ogden, Numerical solution of finite geometry boundary-value problems in nonlinear magnetoelasticity, Int. J. Solids Struct. 48 (2011) 847–883.
[5] S.V. Kankanala, N. Triantafyllidis, On finitely strained magnetorheological elastomers, J. Mech. Phys. Solids 52 (2004) 2869–2908.
[6] M.R. Jolly, J.D. Carlson, B.C. Muñoz, A model of the behaviour of magnetorheological materials, Smart Mater. Struct. 5 (1996) 607–614.
[7] M. Barham, D.J. Steigmann, M. McElfresh, R.E. Rudd, Finite deformation of a pressurized magnetoelastic membrane in a stationary dipole field, Acta Mech. 191 (2007) 1–19.
[8] G. Gioia, R.D. James, Micromagnetics of very thin films, Proc. R. Soc. London A 453 (1997) 213.
[9] D.J. Steigmann, Equilibrium theory for magnetic elastomers and magnetoelastic membranes, Int. J. Non-linear Mech. 39 (2004) 1193–1216.
[10] G.A. Maugin, Continuum Mechanics of Electromagnetic Solids, North-Holland, Amsterdam, 1988.
[11] D.J. Steigmann, A concise derivation of membrane theory from three-dimensional nonlinear elasticity, J. Elasticity 97 (2009) 97–101.
[12] M.E. Gurtin, An Introduction to Continuum Mechanics, Academic Press, Orlando, 1981.
[13] C. Truesdell, R. Toupin, The classical field theories, in: S. Flügge (Ed.), Handbuch der Physik, vol. III/1, Springer, Berlin, 1960.
[14] A. Kovetz, Electromagnetic Theory, Oxford University Press, 2000.
[15] W.F. Brown, Magnetoelastic Interactions, Springer, Berlin, 1966.
[16] A. DeSimone, P. Podio-Guidugli, On the continuum theory of deformable ferromagnetic solids, Arch. Ration. Mech. Anal. 136 (1996) 201.
[17] D.J. Steigmann, On the formulation of balance laws for electromagnetic continua, Math. Mech. Solids 14 (2009) 390–402.
[18] A. Nobili, A.M. Tarantino, Magnetostriction of a hard ferromagnetic and elastic thin-film structure, Math. Mech. Solids 13 (2009) 95–123.
[19] M. Barham, D. White, D.J. Steigmann, Finite-element modeling of the deformation of magnetoelastic film, J. Comput. Phys. 229 (2010) 6193–6207.
[20] R.D. James, Configurational forces in magnetism with application to the dynamics of a small-scale ferromagnetic shape memory cantilever, Continuum Mech. Thermodyn. 14 (2002) 55–86.
[21] R.J. Knops, E.W. Wilkes, Theory of elastic stability, in: S. Flügge (Ed.), Handbuch der Physik, vol. VIa/3, Springer, Berlin, 1963.
[22] R.W. Ogden, Non-linear Elastic Deformations, Dover, NY, 1997.
[23] Q.-S. Zheng, Theory of representations for tensors: a unified invariant approach to constitutive equations, Appl. Mech. Rev. 47 (1994) 545.
[24] R.W. Ogden, Waves in isotropic elastic materials of Hadamard Green or harmonic type, J. Mech. Phys. Solids 18 (1970) 149–163.
[25] A.C. Pipkin, The relaxed energy density for isotropic elastic membranes, IMA J. Appl. Math. 36 (1986) 85.
[26] E. Haseganu, D.J. Steigmann, Analysis of partly wrinkled membranes by the method of dynamic relaxation, Comput. Mech. 14 (1994) 596–614.
[27] A. Atai, D.J. Steigmann, Coupled deformations of elastic curves and surfaces, Int. J. Solids Struct. 35 (1998) 1915–1952.
[28] D.J. Steigmann, Eliza Haseganu's analysis of wrinkling in pressurized membranes, in: A. Guran, A.L. Smirnov, D.J. Steigmann, R. Vaillancourt (Eds.), Advances in the Mechanics of Solids, in memory of E.M. Haseganu, vol. 15, World Scientific, Singapore, 2006, pp. 3–16.
[29] D.J. Steigmann, Tension-field theory, Proc. R. Soc. Lond. A 429 (1990) 141–173.
[30] S.A. Silling, Phase changes induced by deformation in isothermal elastic crystals, J. Mech. Phys. Solids 37 (1989) 293–316.
[31] M. Taylor, D.J. Steigmann, Simulation of laminated thermoelastic membranes, J. Therm. Stresses 32 (2009) 448–476.
[32] W. Hermann, L.D. Bertholf, Explicit Lagrangian finite-difference methods, in: T. Belytschko, T.J.R. Hughes (Eds.), Computational Methods for Transient Analysis, Elsevier, Amsterdam, 1983, pp. 361–416.
[33] P. Underwood, Dynamic relaxation, in: T. Belytschko, T.J.R. Hughes (Eds.), Computational Methods for Transient Analysis, Elsevier, Amsterdam, 1983, pp. 245–265.
[34] S.V. Kankanala, N. Triantafyllidis, Magnetoelastic buckling of a rectangular block in plane strain, J. Mech. Phys. Solids 56 (2008) 1147–1169.
[35] M. Barham, D.J. Steigmann, M. McElfresh, R.E. Rudd, Limit-point instability of a magnetoelastic membrane in a stationary magnetic field, J. Smart Mater. Struct. 17 (2008) 6–11.